npj | flexible electronics

Review article

Published in partnership with Nanjing Tech University

https://doi.org/10.1038/s41528-024-00298-z

Stretchable liquid metal based biomedical devices

Yifan Deng[1], Fan Bu[1,2], Yujie Wang[1], Pei Song Chee[3] ✉, Xiangye Liu[1,2] ✉ & Cao Guan[1,2] ✉

Pursuit of improved living quality has stimulated great demand for high-performance conformal healthcare devices in modern human society. However, manufacturing of efficient, comfortable and stretchable biomedical apparatus faces huge challenges using traditional materials. Liquid metals (LMs) show remarkable potential to solve this problem due to their extraordinary biocompatibility, stretchability, thermal and electrical conductivity. In recent years, tremendous explorations have attempted to make stretchable biomedical devices with LMs. Herein, we review the stretchable LM-based biomedical devices on the topics of disease treatment and human function augmenting. The representative and up-to-date neural interfaces, alloy cement, e-vessels, soft heaters, exoskeletons, and e-skins are summarized. The existing issues of LMs applied for biomedical devices are also discussed. This review can provide guidance for the follow-up research in LM-based biomedical devices.

Increasing demands for high living qualities raise the requirements for improved healthcare in modern society. As a supplementary approach to disease treatment, wearable and implanted biomedical devices arouse intense interest in clinical medicine[1–3]. To develop versatile and comfortable electronic biomedical devices, tremendous research efforts have been devoted to exploiting various kinds of functional materials, such as metal foils[4], carbon-based nanomaterials[5–7], metal-based nanomaterials[8], hybrid nanocomposite[9,10], conductive polymers[11,12], Si-based semiconductors[13], etc. [14] These materials have been widely used in bone repairment, material package, sensor fabrication and other fields[15–17]. Additionally, more innovative methods were introduced to modify the materials and devices[18]. However, traditional materials have several limitations in stretchable biomedical devices. Most metal foils and their alloys exhibit high elastic modulus[19], making them inflexible and cannot fit the movement of the human body. Most of the conductive polymers and carbon-based nanotubes have the potential toxicity, poor ductility and incompatible mechanical strength with humans[20–23]. Synthesis of metal-based nanoparticles is costly, and it is also difficult to control the size and shape of the particles. Moreover, metal-based nanoparticles may also have biotoxicity, and the high degradation resistance of metal-based nanoparticles is also detrimental to the environment[23,24].

To satisfy the requirements of good stretchability and good electrical conductivity simultaneously, liquid metals (LMs) are regarded as the candidates for the design of high-performance electrical devices. The LMs with low melting points generally consist of only a certain range of elements. For instance, Hg, which serves as a part of the traditional thermometer, is the most common LM in daily life. However, the toxicity of Hg results in poor biocompatibility[25]. Besides, alkali metal elements like Rb have very low chemical stability[26]. Recently, Ga- and Bi-based LMs have attracted extensive research interest due to their excellent mechanical and chemical properties.

Unlike Hg and Rb, the Ga- and Bi- alloys show near zero vapor pressures at room temperature[27,28], so there is no worry about Ga or Bi evaporating into humans, and destroying the nervous system as does Hg vapor. Moreover, the Ga and Bi-based LM devices exhibit huge potential in biomedical applications, owing to their marvelous biocompatibility[29–34], stretchability[35–37], high thermal[38–45] and electrical[36,46] conductivity. Thus, they have been intensely investigated recently. For instance, scientists have fabricated LM electrodes used in many basic electronic devices[47], such as capacitors[48,49], inductors[49–51], memristors[52–54], and optoelectronic devices[55–57], achieving good performances in electrical biomedical facilities. Moreover, LM-based devices, such as bone cement, e-vessels, and exoskeletons, can excellently conform with human movement, due to their superior stretchability performance. Besides, LM-based materials can also be used in non-electrical equipment, like drug carriers[58]. Recently, LM-based materials have been widely applied in biomedical fields, such as digestive tract contrast agents[59], nerve repairment[60–62], and sensors[63–68]. (Fig. 1). Although several reviews focus on the properties[69], the biomaterial

[1]Institute of Flexible Electronics, Northwestern Polytechnical University, Xi'an 710072, China. [2]Key Laboratory of Flexible Electronics of Zhejiang Province, Ningbo Institute of Northwestern Polytechnical University, Ningbo 315103, China. [3]Lee Kong Chian Faculty of Engineering and Science (LKC FES), Universiti Tunku Abdul Rahman (UTAR), Sungai Long 43000, Malaysia. ✉e-mail: cheeps@utar.edu.my; iamxyliu@nwpu.edu.cn; iamcguan@nwpu.edu.cn

Fig. 1 | The biomedical applications and challenges of LMs. The biomedical applications include therapy and human function augmenting, but the high cost and corrosivity limit the wide spread of LMs.

application[70], manufacture and modification methods[71,72] of LMs were proposed these days, there is a lack of comprehensive review on the stretchable LM-based biomedical devices with an emphasis on human therapy and function augmenting.

In this review, we focus on the applications of LM-based materials in stretchable biomedical devices. The basic properties of LMs will be first introduced. Then, we will discuss the recent development of LM-based materials applied in biomedical, including human therapy and human function augmenting. Finally, the existing challenges and future prospects of LM-based biomedical applications will be outlined.

Overview Of Lm

Before the elaboration on the application of LMs in biomedical devices, a brief introduction of the LMs and their material systems assists the understanding of the limitations in device manufacturing and the existing challenges. Herein, we emphasize the architecture, manufacturing and modification of LMs as follows.

Architecture

Various architectures of LMs have different application scenarios. For example, the LM-based microfluid can be utilized in nerve repairment, while LM-composites can be used to manufacture bone-cements and exoskeletons[73,74]. Herein, we focus on the LM-based composites, microfluids and printed particles to introduce the structure of the LMs.

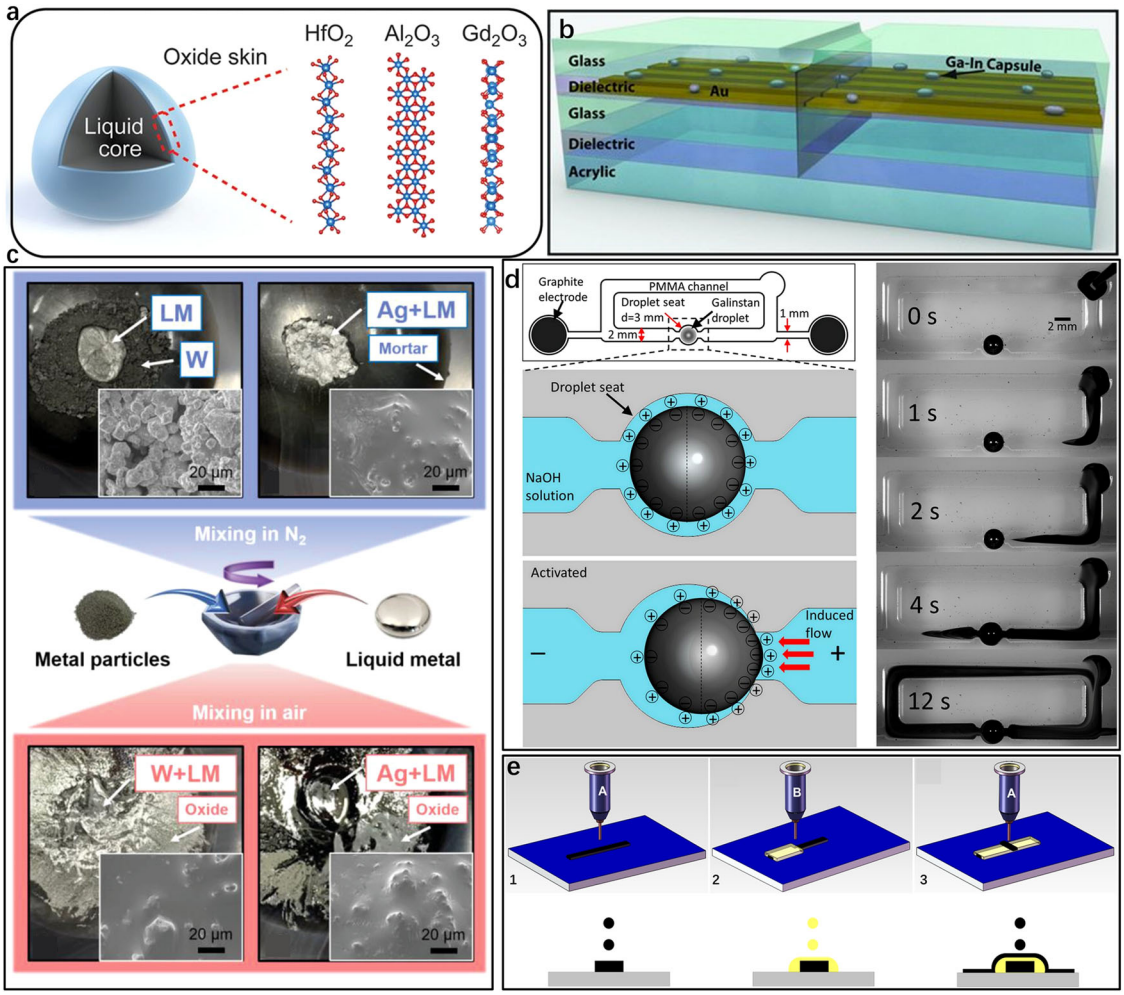

Fig. 2 | The architecture of LMs. a The sketch of LM composites with a core-shell structure[75]. Copyright 2017, Science. **b** The sketch of LM-polymer composites[76]. Copyright 2011, John Wiley and Sons. **c** The schematic graphs of LM particles[78]. Copyright 2019, John Wiley and Sons. **d** The LM- microfluid[83]. Copyright 2014, National Academies Press. **e** The process of printing LMs[95]. Copyright 2013, Springer Nature.

LM composites, in collaboration with other materials, present promising solutions with vast potential for both fundamental research and practical applications. As illustrated in Fig. 2a–c, the basic composite strategies are categorized into three groups: LM composites with a core-shell structure[75], LM-polymer composites[76], and LM-particle composites[77,78]. The functions of these composite strategies are exemplified through typical applications in several key fields. The controlled integration of base LM with functional materials, such as metal nanoparticles, polymers, and drug molecules, allows for precise tuning of LM's intrinsic properties. This tunability opens up significant opportunities to address challenging issues across various sectors, including thermal management, biomedicine, chemical catalysis, flexible electronics, and soft robotics[79].

Microfluids, which involve the integration of functional fluids into a chip-like system with a compact size and low energy consumption for portable applications, hold great promise in areas such as drug/cell screening, sensing, health monitoring, and microfabrication. The substitution of traditional fluids with LMs introduces additional capabilities to the system, shifting its applications beyond bio-related fields to electronics and related domains (Fig. 2d)[70,80–83]. LMs offer distinct advantages in LM-based microfluidics. Firstly, LM can maintain electrical continuity even under significant deformations. Secondly, LM readily forms alloys with various metals, facilitating direct electrical connections between LM-based electronics and substrate materials, including other electronic components. Thirdly, LM wets and fills channels despite its high surface tension, owing to the rapid oxidation of the gallium-based LM surface, forming a self-limiting gallium oxide skin that is a few nanometers thick. This skin possesses low surface tension while exhibiting high affinity and adhesion to various substrates. The combination of conductivity and deformability in LM opens up the possibilities in electronics, enabling soft, flexible, stretchable, reconfigurable, and even self-healable features[84–86]. To date, LM-based microfluidics have demonstrated excellent performance in soft, flexible, and wearable electronics[87], soft robotics[88], biomedical sensors[89], and transient circuits[90]. Additionally, the generation and manipulation of microdroplets play a crucial role in microfluidics research. The fabrication of LM droplets and their dispersion in elastomers has advanced in recent years. Microdroplet composites, derived from these advancements, find significant applications in the fields of electricity, heat, mechanics, and supercooling. Therefore, beyond filling the LM continuous phase in microfluid chips, the study of LM microdroplets/composites is closely interconnected with the field of LM microfluidics.

With the advent of the information age, electronic products are playing an increasingly crucial role. In recent decades, various electronic manufacturing methods have been extensively explored[91–93]. LM printed electronic (LMPE) (Fig. 2e) is one of the most cutting-edge materials for solving the issue of low conductivity of the traditional inorganic nanomaterials[94,95]. From both theoretical and technical perspectives, LM is a highly desirable choice for preparing electronic inks due to its high charge mobility (up to 106 S m^{-1}) and adjustable physical and chemical properties[90,96], such as low melting point, high thermal conductivity, and electrical conductivity. The fundamental principles and practical technologies for molding LM electronic inks and printers have been established. A group of LMPE equipment, inks, and application products like electronic skins has even transitioned into the industry, witnessing rapid industrialization in the field. LMPE has garnered widespread attention from academia to industry, indicating a bright future in the biomedical field[97].

Manufacture and modification

LMs demonstrate their outstanding properties in various fields, while the processes of manufacture and modification affect the performances of LM-based facilities, such as chemical and electric stabilities, thermal sensitivity, anti-bacterial ability, viscosity, biocompatibility, and magnetism[72,98,99].

Magnetic LMs (MLM) are introduced to have a better simulation of the dynamic stiffness change. For example, Li et al.[74] proposed a methodology to synthesize the MLM which could be applied in bone repair. The magnetic silicon particles (Fe@SiO_2) were added into the prepared Galinstan (special weight percent: Ga 68.5%, In 21.5%, and Sn 10%), and the mixture will be stirred to guarantee homogeneous distribution of the Fe@SiO_2. The as-fabricated MLM has a good ability to respond to the changes in the external magnetic field by simulating the regeneration of bones.

Moreover, several fabrication methods of non-wettable and non-sticky LM marbles (LMMs) were designed to address the stickiness problem of oxidized LM alloys exposed to the air. In 2018, Chen et al.[100] proposed a nonsticky LM droplet with coated graphene shells. As illustrated in Fig. 3a, the LM droplets were dropped and rolled on the graphene sheets. Due to the adhesion between the oxidized LM layer and the graphene sheet, the LM droplet was packed by a nest-like graphene cover (Fig. 3b).

The galvanic substitution surface modification occurs, owing to the difference of the electrochemical potential gradient between the two metals/metal ion pairs, which not only assists in enhancing the photothermal conversion efficiency of LM nanoparticles (NPs)[101] but also improves the catalytic activity in certain areas[102]. For example, Guo et al.[101] proposed an in-situ interfacial galvanic substitution reaction to prepare the heterogeneous eutectic gallium indium-Au (EGaIn-Au) nanoparticles. As shown in Fig. 3c, the $HAuCl_4$ solution was added into the EGaIn-Au nanoparticles suspension, triggering the in-situ growth of the Au-coated shell. The photothermal performance test demonstrated its excellent behavior in thermotherapy on cancer treatment.

Post-synthetic strategies were also adopted for core-shell structural modification of LMs. Figure 3d illustrates a synthesis method for ZrO_2-covered EGaIn nanoparticles, which exhibits enhanced efficiency in internalizing into cells[103]. Zheng. et al.[104] elucidated a route for the synthesis of a conductive LM-based core-shell particle that could be used to fabricate self-repairing soft circuits. The silver encapsulates the LM particles via screen printing, and the whole material shows remarkable resistance stability ($\Delta R/R_0 < 1.65\%$ after 10,000 bending cycles). Furthermore, the silica coating strategy also enhances the thermal stability and chemical stability of LM NPs[105] (Fig. 3e).

Polymers, which have strong intra- and inter-molecular interactions, are utilized for encapsulating LMs which raises scientists' interest these days. Figures 3f and 4a show the common methodologies for polymer encapsulation, including sonochemical assembly[106], chemical-initiated crosslinking polymerization stragedy[107], and atom transfer radical polymerization (ATRP)[108]. For example, Li et al.[109] utilized aqueous ultrasonication to prepare the marine polysaccharide-wrapped LM, and the alginate assisted in the downsizing and formation of microgel shells for EGaIn droplets (Fig. 4b). Thrasher and his team proposed a photo-initiated polymersation for encapsulation[110]. The poly-LM networks exhibited an outstanding performance in resistance stability over large strains. Moreover, the reversible addition-fragmentation chain-transfer (RAFT) polymersation[111] and the ring-opening polymersation[112] also serve as the LM modification strategy.

To enhance the behavior in biocompatibility, several bioengineering modification methods were proposed ingeniously[113]. For instance, Xu et al.[114] designed enzyme-coated LM-based nanobots utilized in bio-imaging (Fig. 4c). Firstly, the LMs were sonicated in the dopamine solution to synthesize the polydopamine-based LM NPs. Then urease and cefixime trihydrate were loaded and the enzyme was finally coated at the surface of LM NPs with the assistance of a glutaraldehyde linker through electrostatic adsorption. Similarly, Fig. 4d illustrates a cell membrane-coating strategy for surface engineering[115], which improved the anti-tumor ability of the LM NPs.

Generally, various surface engineering methods have been exploited to construct protective layers for LM improving the performances of LM-based nanomaterials. This modification enhances the chemical stability and biocompatibility of LM-based materials, enabling their wider applications in the fields of biology, energy, the aviation industry, and other scenarios. However, several LM-based materials are difficult to apply on a large scale due to the complexity and high cost of the preparation methods. Therefore, there is an urgent need for scientists to further invent more low-cost production processes for LM materials.

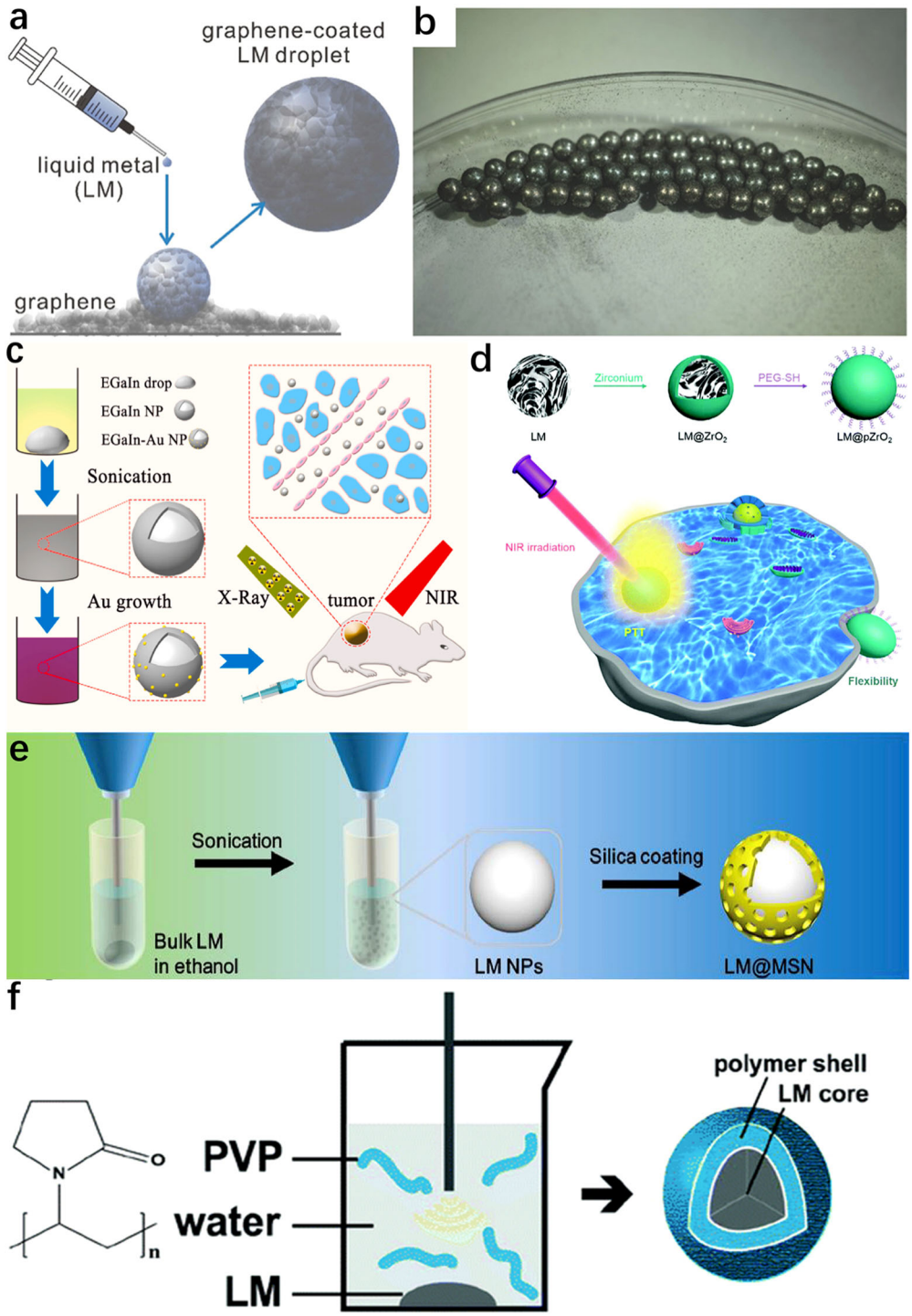

Fig. 3 | The fabrication and modification of LMs. a The coating procedure of graphene sheets[100]. Copyright 2018, John Wiley and Sons. **b** A photograph of the graphene-coated LM droplets[100]. Copyright 2018, John Wiley and Sons. **c** The preparation and application of the galvanic substitution method modified EGaIn-Au NPs[101]. Copyright 2021, Elsevier. **d** The synthesis process of LM@pZrO$_2$ NPs and the flexibility under scheme[103]. Copyright 2009, Royal Society of Chemistry. **e** Preparation of LM@MSN[105]. Copyright 2019, Elsevier. **f** Fabrication of LMs based on sono-chemical assembly modification[106]. Copyright 2009, Royal Society of Chemistry.

Properties Of Lm

To understand why LMs are qualified for biomedical devices, being acquainted with their basic properties is of great significance. The biocompatibility of the materials ranks first when being used for the manufacturing of biomedical devices. Moreover, good chemical stability is critical to avoid generating potentially toxic substances. Table 1 compares the different properties between LMs and other biomedical materials, indicating the potential advantages of LMs in the field of biomedical devices. Due to high fluidity[35,116,117], low viscosity[118–120], low melting point[121], and special crystallinity[122], LMs and LM composites show good stretchability, which endows biomedical devices with good fit for human movements. Along with the properties mentioned above, the excellent electrical conductivity of LM

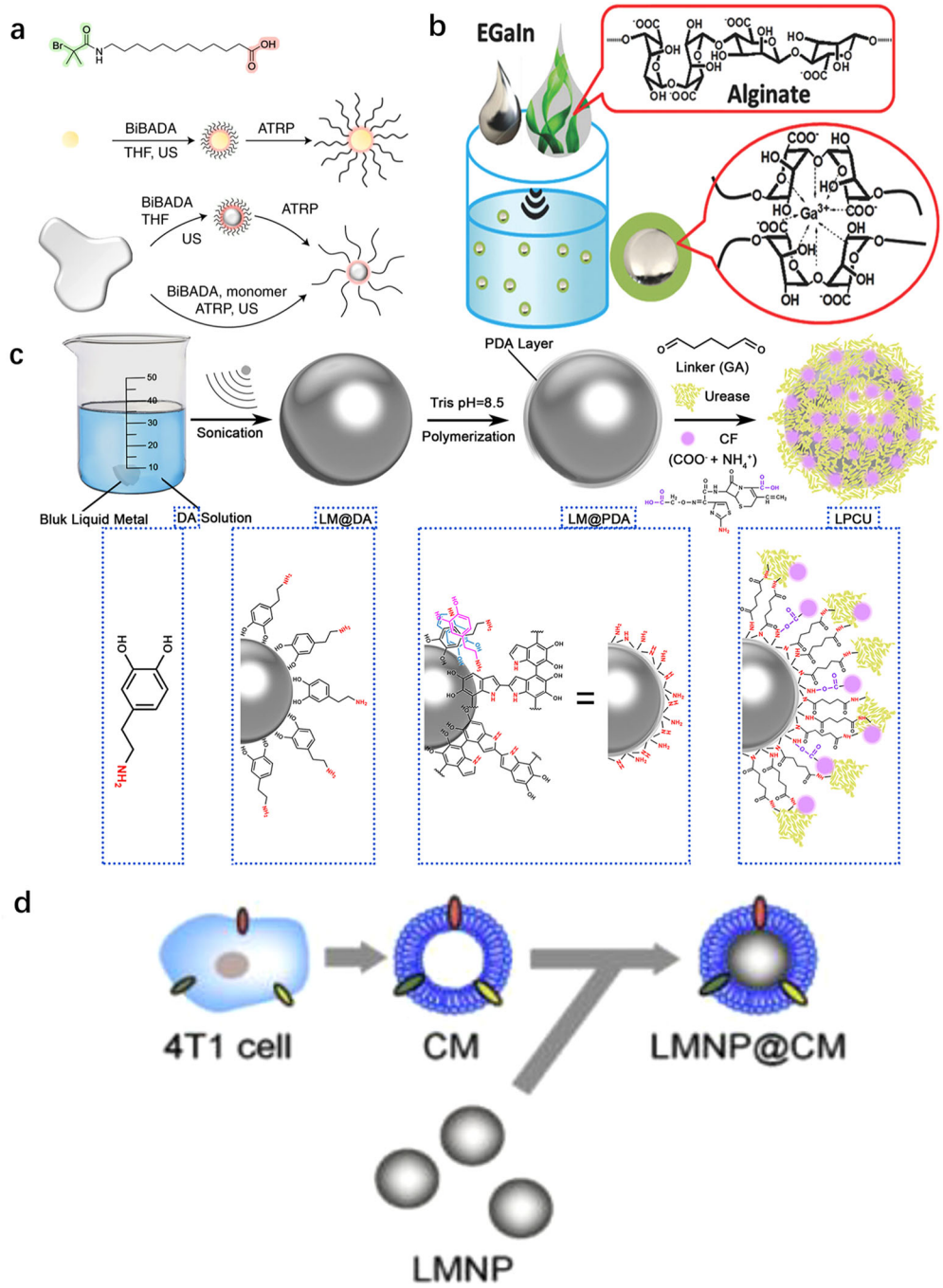

Fig. 4 | The fabrication and modification of LMs. a The structure and modification process of ATRP[108]. Copyright 2019, Springer Nature. **b** The sonicating and encapsulating procedure of EGaIn[109]. Copyright 2018, John Wiley and Sons. **c** The synthesis process of enzymatic LM nanobots[114]. Copyright 2021, American Chemical Society. **d** The manufacture of LMNP@CM[115]. Copyright 2020, John Wiley and Sons.

ensures its applications in electrical equipment[68,123]. Herein, we elucidate the characteristics of biocompatibility, chemical stability, stretchability, and conductivity of LMs before overviewing their biomedical application.

Biocompatibility

Ga-based and Bi-based alloys are two kinds of common LMs in the healthcare field. In the past few years, bio-safeties of LM-based materials have been widely tested through both in vitro and in vivo experiments. Various categories of LMs and LM alloys have different toxicity. Sano et al.[124] carried out a study of the direct toxicity of Bi. They selected enough male and female Crj:CD (SD) IGS rats (SPF) and then divided them into two experiments. One group of rats was studied for acute oral toxicity with a dose of 0 and 2000 mg kg^{-1}, and the other group was used to unveil the potential toxic effect of Bi, where the rats were administrated orally at a dose of 0, 40, 200, and 1000 mg kg^{-1} daily for 4 weeks. The relevant parameters were detected. As illustrated in Fig. 5a–d, there was no significant difference among each group. Even high Bi dose (1000 mg kg^{-1}) orally administrated rats shared similar necropsy and histopathological findings with those at the dose of 0 mg kg^{-1} (Table 2). The results showed that neither the acute nor long-term oral administration led the adverse reactions in rats. The lethal dose 50% mortality rate dosage of Bi turned out to be higher than 2000 mg kg^{-1} for the rats, so the toxicity of bismuth is much lower than Hg. However, the inorganic Bi compounds have the potential to be adsorbed and diffused in human organisms[125], and administrating the Bi compounds

Table 1 | Chemical, mechanical, and electrical properties of different biomedical materials

Materials	chemical stability	Stretchability	Resistance stability	Stiffness	Biocompatibility
LM-based elastomer	Oxide layer-low reactivity Metal-high reactivity[37,79]	78%[79]	ΔR/R = 2%[79] (70% strain, 1000 cycles)	1.11 MPa[79]	Low interactions with biological tissues and low toxicity[37]
Metal film	Easy oxidation[214,215]	55%[214]	ΔR/R = 30%[214] (20% strain, 10,000 cycles)	-	Exist potential cytotoxicity to human cells[215]
Carbon-based nanomaterials	Low reactivity[216,217]	200%[216]	ΔR/R = 80%[216] (60% strain, 1000 cycles)	-	More biocompatible and less cytotoxic with chronic effects[217]
Metal-based nanomaterials	Low reactivity[217,218]	70%[218]	ΔR/R = 80%[218] (70% strain, 1000 cycles)	3.2 MPa[218]	All metal NMs induce an inflammatory response[217]
Hybrid nanocomposite	Depends on materials and conditions[219–221]	50%[219]	ΔR/R = 400%[219] (40% strain, 1000 cycles)	0.6 Mpa[219]	Depends on material selection and conditions[220,221]
Conductive polymers	Undergo oxidation or reduction[222,223]	1,800%[222]	ΔR/R = 170%[222] (300% strain, 4 cycles)	1.86 MPa[222]	Obstruction of blood vessel formation[223]

will cause acute renal failure[126]. Therefore, a longer in vivo toxicity investigation of bismuth is of great significance to further determine the relationship between the safe concentration threshold of bismuth.

Ga-based materials are another mainstream LM. Recently, many researchers have focused on the cytotoxicity of Ga. For example, Liu et al.[59] found that Ga was a potential digestive tract radiography agent and conducted the safety test simultaneously. They separated 10 rats into two groups randomly, where the rats in the experimental group were given 0.2 mL Ga while the control group received deionized water by gavage. Then the rats were utilized for histological and basic indexes observations. The data of the two groups can be regarded as the same, verifying the biocompatibility of Ga. Moreover, not only do Ga and Bi have low cytotoxicity, but piles of experiments also demonstrated the safety of Ga-based and Bi-based alloys[127–130]. Nonetheless, the Ga-based LMs will get oxidation into gallium oxide hydroxide (GaOOH) in an oxygenated high-temperature atmosphere, and the toxicity of GaOOH limits the practical application of Ga-based biological devices[131].

Additionally, to investigate the cytotoxicity of the ions released from eutectic gallium-indium alloy (EGaIn) on human cells. Kim et al.[132] conducted a toxicity test of EGaIn in an aqueous environment. The results revealed that although mechanical agitation would augment the cytotoxicity, EGaIn could be generally considered safe in a normal aqueous environment. Furthermore, although organometallic compounds are summarized as more toxic generally[133], many experiments indicate their good biocompatibility[116,134–137]. However, it should be noted that Sn and many Sn salts have low cytotoxicity, while many organotin compounds harm the nervous system[133].

With the development bio-application of LM NPs[138], the toxicity aroused scientists' attention. For example, Narayanasamy et al.[139] reported that the prolonged-acting, muti-targeting Ga-based NPs helped inhibit human immunodeficiency virus (HIV) infection. And there was no observation about macrophage cytotoxicity caused by the Ga-NPs in 24 h. Moreover, Lin et al.[140] prepared poly (1-octadecene-alt-maleic anhydride) (POMA) grafted LM NPs and investigated their toxicity. The Chinese hamster ovary (CHO) cells were exposed to LM NPs. The results showed the low cytotoxicity of LM NPs under the concentration of 62.5 μg mL^{-1}.

Furthermore, the environmental impact of LMs cannot be ignored. Yu et al.[141] reported the environmental pollution effects of Ga. As illustrated in Fig. 6a, due to low solubility in water, Ga has a low concentration in the daily aquatic environment. However, the Ga levels in inhalable gas samples are quite higher in manufacturing areas (Fig. 6b). Similarly, the inhalable gas levels of Bi in the workplace are also high, which has caused a few bismuth poisoning events[142]. Besides, Ga may be oxidized to GaOOH in an aqueous environment[131], which decreases the biocompatibility of the LM-based devices. Despite the direct pollution caused by the bulk LMs, the environmental impact of Ga and Bi-based LMs is much lower than lead and Hg[142]. Moreover, the scientists also devoted themselves to investigating the modification methods that decrease the pollution of LM-based materials. For example, Mao et al.[143] proposed a nanocellulose-based LM circuit, which is soluble in water and the LM ink could be recycled conveniently.

In summary, with excellent biocompatibility, many Ga-based and Bi-based LMs are relatively safe to be utilized for biomedical devices. Nevertheless, further investigations are needed to determine the toxicity and pollution of LM-based materials.

Chemical stability

Owing to the high reactivity of Ga, LMs containing Ga are easily oxidized in humid air, which can improve the stability of the Ga-based alloy by forming an inactive oxidation layer. Scharmann et al.[144] found that regardless of low or high relative humidity for a short or long period, the oxidized Ga (Ga_2O_3 mostly, which is stable) mainly scattered at the surface, and the Ga atoms dispersed in the deeper inside, while Sn and In were predominantly stable. However, in a humid environment, the liquid Ga tends to be over-oxidized and transform to a crystalline structure (GaOOH, which can serve as a catalyst) when the Ga-based LMs are heated to 343 K[145,146]. Inversely, the Ga

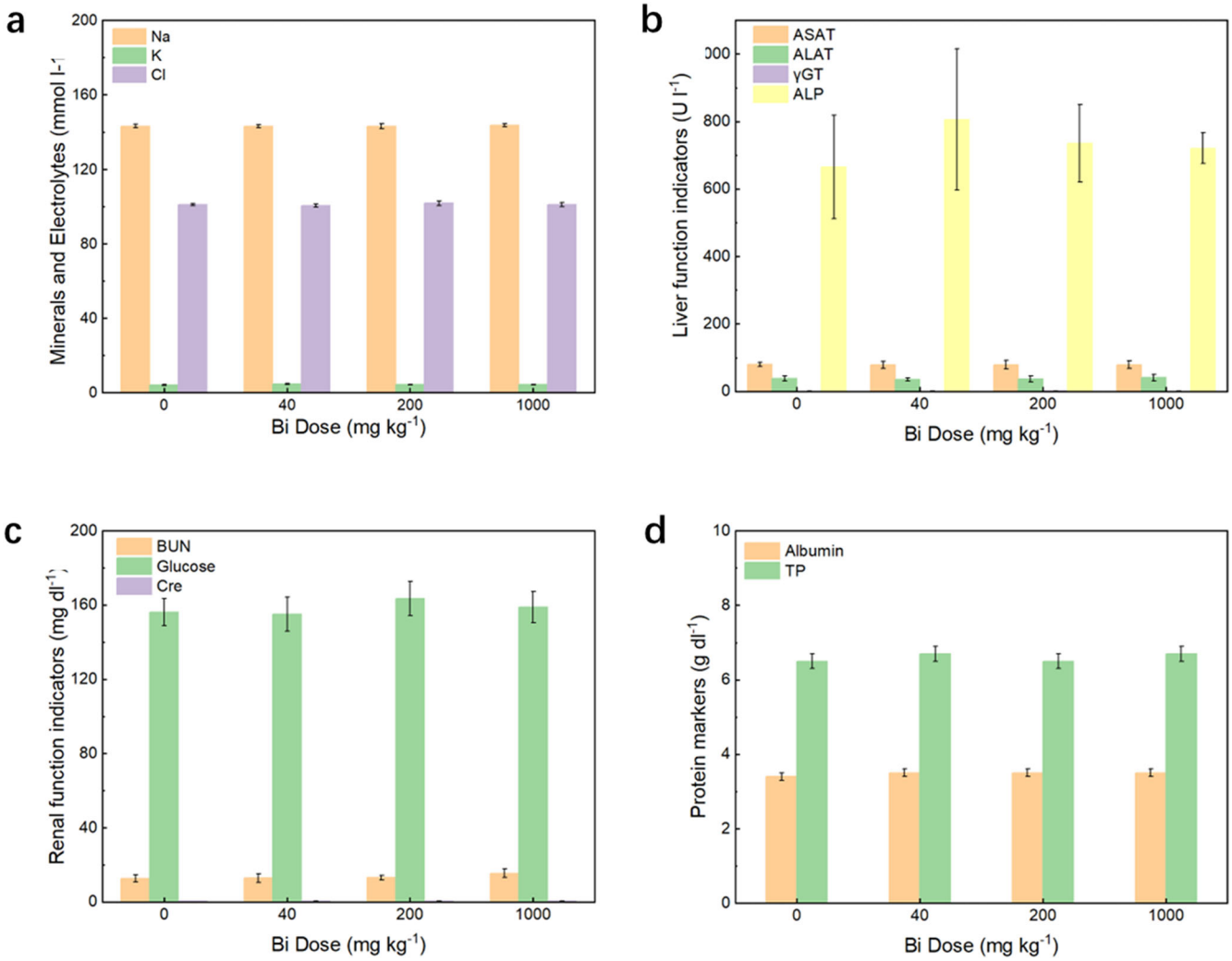

Fig. 5 | Biotoxicity test of Bi with different doses[124]. **a** Minerals and Electrolytes of rats under different Bi Dose concentrations. **b** Liver function of rats under different Bi Dose concentrations. **c** Renal function of rats under different Bi Dose concentrations. **d** Protein markers of rats under different Bi Dose concentrations. **a**–**d** The error bars show the standard deviation.

oxide layers could also be reduced under negative potential or in an acid or base environment[147]. Moreover, Ga would react with other metals (like Cu) in the LM-based devices due to its high reactivity. For example, HerØ et al.[148] studied the long-term corrosion of Ga alloys in vivo. They tested GF (65% Ga, 19% In, 16% Sn), Galloy (62% Ga, 25% In, 13% Sn, 0.05% Bi) and EGaIn (75.5% Ga, 24.5% In). The samples were exposed to the oral cavity for 2–9 months. The scanning electron microscopy results showed that the $CuGa_2$ phase corroded the most substantially in the three alloys. Compared with other alloys, Galloy was less corrosive, indicating that modifying the microstructure of LM-based alloys helps improve the corrosion resistance.

On the other hand, scientists have developed various LM composites to enhance stability. For example, Li et al.[109] introduced a method to fabricate a biocompatible aqueous ink, which was manufactured by introducing the EGaIn into marine polysaccharides microgels, reinforcing the stability of LM composites. Furthermore, Wu et al.[149] proposed a Ga-Mg alloy which has the potential to act as a biodegradable material, where Ga was modified and utilized to decrease the degradation rate of Mg in body fluid. Therefore, the corrosivity of gallium could be reduced.

Moreover, increasing investigations focus on the rupture of LM-based NPs. Liu et al.[150] prepared a series of polyurethane-based LM NP materials (Fig. 7a) and investigated the rupture stress by numerical calculations together with experiments. Researchers stretched the polyurethane-based LM NP materials cyclically, and Fig. 7b–e illustrated that the smaller NPs had higher activation strain and were less likely to rupture. When the oxide layer breaks, the LM exudation will cause the insulation surfaces to be electrically conductive, which may have potential harm to human bodies and limit the application of LM-based biomedical devices.

Overall, although the performance of LMs might degrade in high temperatures or the acid or base environment, various modification methods assist in enhancing their chemical stability naturally or artificially, both of which enable LM-based devices with long working life. Nonetheless, further investigations about how to optimize the performance of LM-based devices are required. Moreover, more research is needed to understand the effect of the effusion of LM when the gallium oxide shell is ruptured because of the device's deformation.

Stretchability and electrical conductivity

The good stretchability of a biomedical device enables a long operating life and improved adaptability to the human body. It is nonsensical to only discuss flexibility while ignoring changes in electrical conductivity for materials. Therefore, researchers often analyze stretchability, conductivity, and resistance stability simultaneously.

The LMs with high flexibility are suitable for basic biomedical device application[151–155]. Tang et al.[116] introduced a printable metal-polymer conductor (MPC). As illustrated in Fig. 8a, the LM particles were embedded in the polymer matrix. Not only did the MPC maintain approximately 30% of

Table 2 | Histological findings within the 28-d perennial oral dose toxicity study[124]

Bi Dose Animal Number	0 mg kg^{-1} 6 Male	1000 mg kg^{-1} 6 Male	0 mg kg^{-1} 6 Female	1000 mg kg^{-1} 6 Female
Heart				
Myocardial degeneration/ Focal fibrosis	1	1	0	0
Liver				
Microgranuloma	1	2	2	1
Focal necrosis	0	0	1	0
Kidney				
Proximal basophilic tubule	4	4	2	2
Cyst	1	0	0	0
Pelvis dilation	1	1	0	0
Hyaline droplet in proximal tubular epithelium	4	5	0	0
Focal interstitial infiltration of lymphocyte	1	1	2	2

Each value is the number of animals with histopathological findings. Significantly different from control: $^{*}p < 0.05$; $^{**}p < 0.001$. ($n = 6$; paired t test).

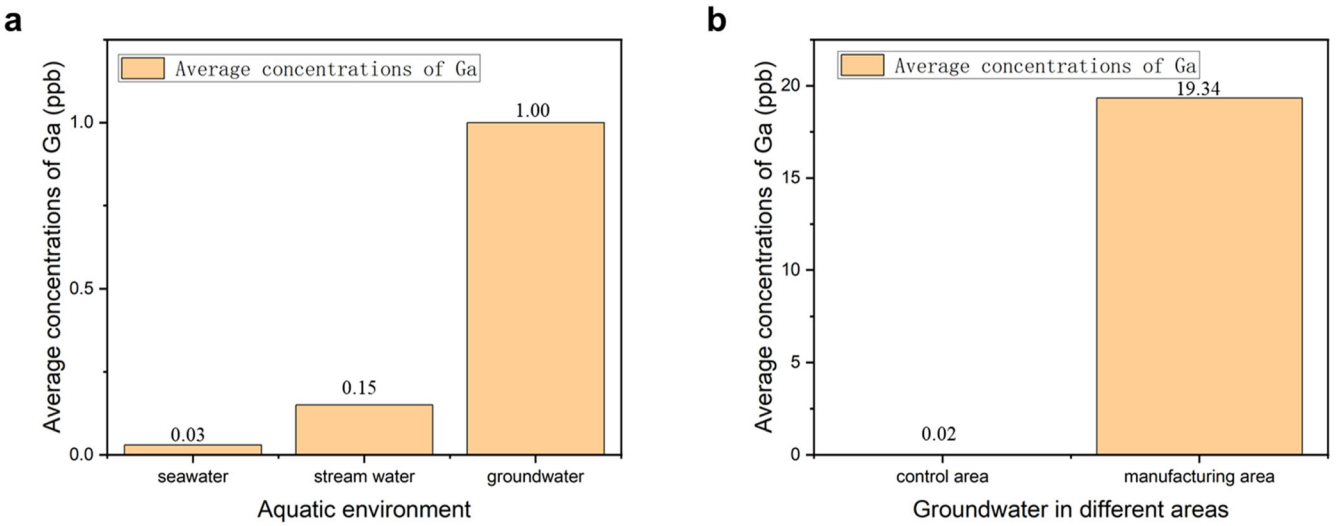

Fig. 6 | Average concentrations of Ga in different area[141]. a The average concentration of Ga in different water resources. The error bars show the standard deviation. **b** The average concentration of Ga in control and manufacturing areas. The error bars show the standard deviation.

its initial conductivity (8×10^3 S cm^{-1}) when subjected to a large strain of 500%, but also a few significant changes in its resistance ($\Delta R/R < 3\%$) were observed after 50% strain for 10,000 cycles (Fig. 8b). Similarly, Wang et al.[117] presented another type of superelastic conductor with an original conductivity of 8331 S cm^{-1}. These highly flexible conductors could be stretched up to 800% for 10,000 cycles, and the resistance increased 8 times compared with the initial one.

Apart from the low Young's modulus of the materials, the structure of the circuit also helps improve the stretchability. For instance, Li and his team proposed annular-shaped branch channels to reinforce the stretchability of LM-embedded elastomeric conductors. As shown in Fig. 8c, the change of resistance stayed below 2% within 1000 cycles under 60% strain. Figure 8d, e show the construction scheme of the LM-based component. Additionally, another structural design strategy was introduced by Thrasher[110]. As demonstrated in Fig. 8f, core-shell shaped LM particles were synthesized with the acrylate ligands, forming polymerized LM networks (Poly-LMNs). The resistance of Poly-LMNs changed about 10% under 100% strain over 10,000 cycles.

Generally, LM-based devices are equipped with both excellent stretchability and good conductivity as well as resistant stability. Their outstanding performances make them to have wide application prospects. However, reliable stability of resistance can only be achieved within a small range of deformation. Therefore, methods to enhance the electrical stability under large-scale strain are required to be investigated in the future.

Therefore, many LM-based conductors are highly durable, exhibit excellent stretchability, and maintain good conductivity after continuous stretching. These advantages make LMs promising candidates for manufacturing flexible electronic biomedical devices.

Applications oriented toward human therapy

Nerve repairment and neural interface

Nerve injury, a challenging condition to cure, affects thousands of patients annually. Unfortunately, current treatment protocols are ineffective in repairing damage to the central nervous system[156]. Additionally, when the nerves are injured, the axons are often stretched over long distances, leading to a lack of contact between tissues and prolonged atrophy of target tissues[157]. Therefore, researchers are actively seeking a method to repair injured nerves efficiently. Fortunately, LMs offer a potential solution to this problem.

Since the 20th century, scientists have been conducting research on neural implants. In 1999, Williams et al.[158] introduced a protocol for recording chronic and multi-site unit data in the cerebral cortex of awake animals over an extended period. This protocol served as a model system for studying the biocompatibility of neural implants and laid the groundwork for future neural implant studies.

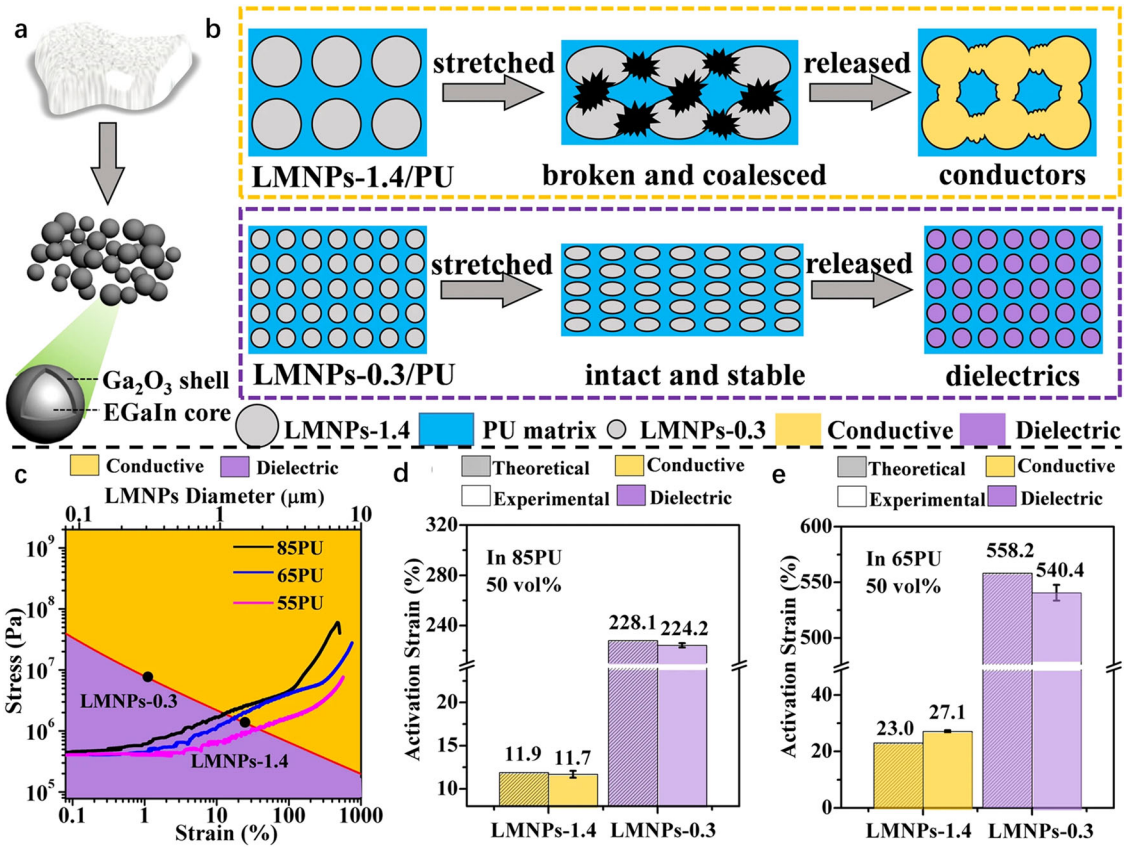

Fig. 7 | The rupture of LM-based NPs. a The design of the polyurethane-based LM NP material[150]. **b** The morphology changes of different polyurethane-based LM NP materials[150]. **c** The stress-strain curves of different polyurethanes coupled with LM NPs activation stress, where the NPs break in the orange area and remain intact in the purple area[150]. **d** The experimental and theoretical activation strain of 50% LMNPs-0.3/85PU (50% vol% LMNPs-0.3 dispersed in 85PU matrix) and 50% LMNPs-1.4/85PU. The error bars show the standard deviation[150]. **e** The experimental and theoretical activation strain of 50%LMNPs-0.3/65PU and 50%LMNPs-1.4/65PU. The error bars show the standard deviation[150]. **a–e** Copyright 2021, Springer Nature.

Over the past decade, many neural experiments utilizing LMs have been carried out. For instance, Jin et al.[135] proposed a method for directly fabricating 3D medical electronic devices in vivo in 2013. They utilized gelatin as the primary packing material with GaInSn alloy inside. Gelatin was injected into porcine tissue, then a mold was filled into the gelatin and removed after shaping. Finally, the LM was injected into the shaped gelatin to form medical electronics (Fig. 9a). The as-formed electrode demonstrated the potential of LMs as an efficient electrocardiograph and stimulator electrode. In the same year, Hallfors et al.[73] depicted a protocol to stimulate neurons together with the subcellular compartments moderately. As illustrated in Fig. 9b–d, LM electrodes were combined with microfluid culture platforms, and these LM electrodes were used to target and depolarize axons, emerging as a useful tool for treating multiple neurological diseases.

Following the initial research, an in vivo experiment was conducted further to explore the potential of LM in the neural application. In 2014, Zhang et al.[159] testified that LM could serve as a medium for transmitting neural signals and stimulating the muscles of frogs. In 2016, Liu et al.[160] conducted experiments on mice, utilizing a combination of liquid gallium (Ga) and silicone rubber tube shells to connect two injured nerves. The electrode connected to the injured nerve exhibited similar outcomes to the uninjured nerves. As a result, the relevant muscles were able to avoid the issue of atrophy. Additionally, a microelectrode array based on LM was introduced in the subsequent year[60]. This flexible array addressed the problem of potential mechanical incompatibility, which is often encountered with traditional rigid stimulating electrodes. Remarkably, even deceased frogs were able to move their legs when implanted with the microelectrode array rhythmically. This advancement in therapy opened up the possibilities for restoring nerve functions.

However, these initial experiments discussed earlier did not involve the complete implantation of peripheral nerve interfaces or the recording of peripheral neural signals. In 2022, Tang et al.[161] fabricated LM-based fluidic cuff electrodes (Fig. 9e) and implanted them into rats for two weeks (Fig. 9f). The results demonstrated that these stretchable nerve cuff electrodes were able to transmit neural stimuli to the peripheral nerve and activate the somatosensory cortex. Importantly, the long-term implantation did not adversely affect the well-being of the rats.

Based on the previous research, it can be concluded that LM-based neural electrodes exhibit excellent biocompatibility and flexibility. Their high conductivity makes them an outstanding signal transmission characteristic. Therefore, LMs are expected to play a significant role in nerve repair, such as in neural prostheses, neural stimulator systems, nerve connection agents, etc.

Furthermore, equipped with good biocompatibility, high conductivity, and good stretchability, LMs can also be used to fabricate neural interfaces. For instance, Dong et al.[162] provided a fabrication strategy to manufacture a stretchable electrode to monitor real-time epileptiform activities. The electrode was compatible with the brain surface and could record the signals. Other researchers have also reported plentiful LM-based neural interface materials fabrication methods[163–167] and devoted themselves to the relevant biological experiments, promoting the development of neural interfaces. In the future, neural interface systems may serve as monitors for human health recording and have the potential to realize the interaction between human beings and electronics. Although a series of experiments are needed to

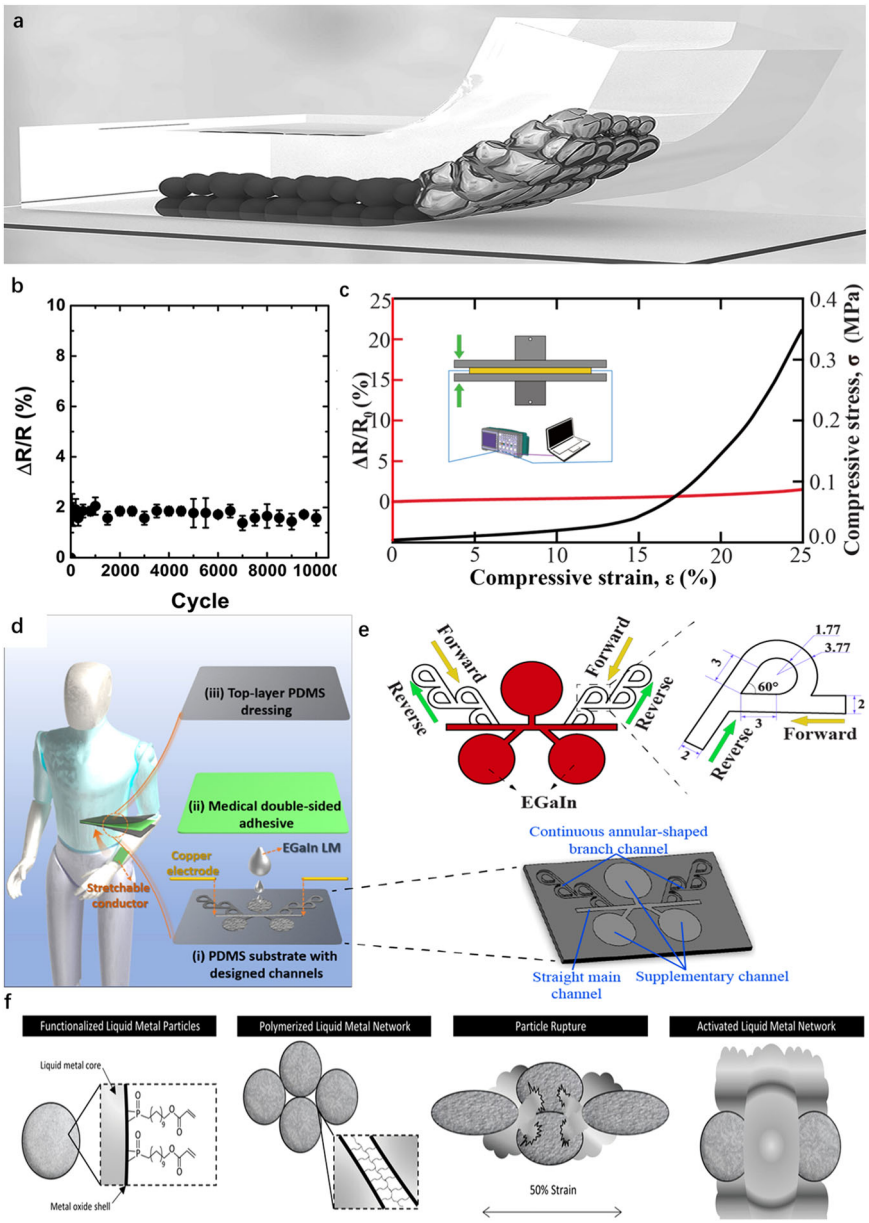

Fig. 8 | The stretchability and electrical conductivity of LMs. a The schematic component of MPC[116]. Copyright 2018, Elsevier. **b** ΔR/R changes with a strain of 50% for 10,000 cycles of MPC. The error bars show the standard deviation[116]. Copyright 2018, Elsevier. **c** Fractional resistance changes of the LM-based elastic conductor with annular-shaped branch channels[79]. Copyright 2023, Elsevier. **d** The scheme of the LM-based elastomer with annular-shaped branch channel[79]. Copyright 2023, Elsevier. **e** The design of the annular-shaped branch channels with continuous performance[79]. Copyright 2023, Elsevier. **f** Formation and activation of polymerized LM networks[110]. Copyright 2019, John Wiley and Sons.

achieve the goal of nerve therapy and neural interface fabrication, LM is undoubtedly a promising material for neurosurgery.

Liquid-solid phase transition alloy cement

On a daily basis, our bodies endure the weight and strain that can cause small cracks in our bones[168]. Remarkably, our bones possess the ability to self-repair, promptly refilling these small cracks before they can cause irreversible damage. However, as we age, the self-repair capability of bones diminishes, making orthopedic diseases such as osteoporosis more common among the elderly. Additionally, the violent impact also leads to fracture. Therefore, using some methods to cover the shortage of self-repairing bones is of great significance due to their structural material function in human bodies.

Polymethyl methacrylate (PMMA) cement and calcium phosphate cement (CPC) are two traditional bone cement used to repair bone defects[169,170]. Nevertheless, these traditional materials have many flaws[171]. For example, during the polymerization process, these materials generate excessive heat and then impair the surrounding tissue, leading to the decreased mechanical properties of bone cement[172]. Moreover, traditional materials do not return to a liquid state after solidification, making their removal challenging. Additionally, the leakage of cement can potentially cause severe cardiac injuries[173]. Therefore, there is an urgent need for new types of bone cement to address these issues. LMs are anticipated to provide solutions to these challenges.

In 2014, Liu et al.[129] proposed a Bi-based liquid-solid transition alloy with a low melting point of 57.5 °C. Unlike traditional PMMA bone cement, which consists of separate powder and liquid systems, the liquid-solid transition alloy only has one system, where the liquid and solid phases can be reversibly transformed. This simplified the complex preparation process. Distinctively, while the solidification of PMMA cement involved a chemical reaction, LM cement relied solely on a physical process. Furthermore, the temperature decreases rapidly from its peak during solidification (Fig. 10a), reducing trauma to surrounding tissues. Surgeons can also preheat the materials at a lower temperature or prechill the prosthesis and the bone cavity before filling to minimize the time spent at high temperatures. This mild thermal effect not only holds the potential to improve repair effectiveness but also lowers the likelihood of premature cement failure. Rapid cement molding can also reduce the incidence of infection during surgery.

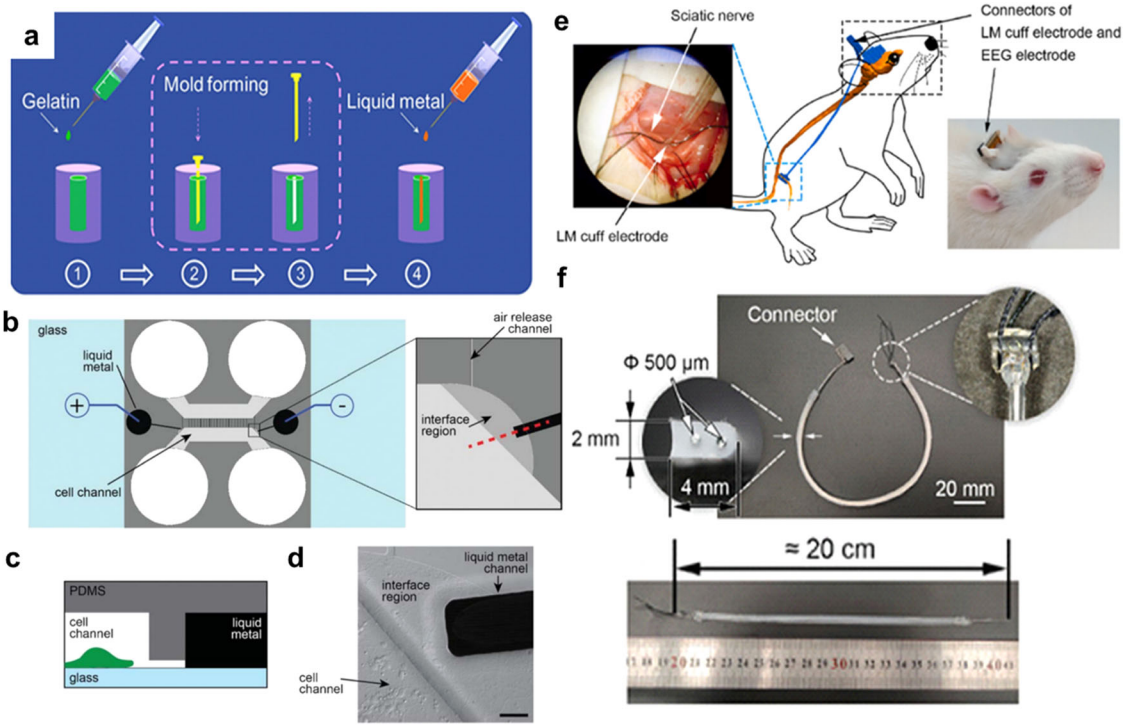

Fig. 9 | LM electrodes for nerve repairing. a Fabrication processes of a 3D medical electronic device[135]. Copyright 2013, Springer Nature. **b** The schematic diagram of the LM-based electrode[73]. **c** The profile view of the red line in *figure b*[73]. **d** The DIM image of the interface region[73]. **b–d** Copyright 2013, Royal Society of Chemistry. **e** Images of an LM-based fluidic cuff electrode[161]. **f** The photographs and schematic of the LM-based cuff electrode in the stretchability test[161]. **e**, **f** Copyright 2022, Elsevier.

However, although LM cement has a higher modulus, it behaves less effectively than acrylic cement in compression and bending strength tests. Therefore, utilizing the LM cement in non-bearing positions might be a more suitable choice. Nevertheless, LM cement performs well in fatigue, crack resistance, and safety tests. Furthermore, with appropriate modifications, LM cement may perform better[174]. Further research on the Bi-based LM demonstrated excellent characteristics in corrosion resistance (Fig. 10b) and a capacity for osseointegration. Moreover, the injected alloy remained immobilized for 210 days[128].

Another LM-based scaffold for bone tissue engineering has been developed to provide a changeable material for bone regeneration. Li et al.[74] introduced magnetic liquid metal (MLM) and porous magnetic liquid metal (PMLM), which could change their shapes by changing the external magnetic field. The MLM scaffold was fabricated by introducing magnetic silicon dioxide particles into Galinstan, while adding polyethylene glycol as a template resulted in the fabrication of the PMLM (Fig. 10c). The result demonstrated that the external magnetic field could change the stiffness of MLM by rearranging the distribution of magnetic particles, which can stimulate the osteogenic differentiation of mesenchymal stem cells. Moreover, as shown in Fig. 10d, other research also reported the rapid cooling property of LM-based bone cement during solidification[175].

Nevertheless, several investigations indicated that the supercooling effect of LM during the solid-liquid phase transition may result in potential side effects on human tissue. For example, Zhang et al.[175] evaluated the negative effects of latent heat from LMs on biological tissues. BiInSn alloy, one of the LM-based bone cement materials, was selected for the test of thermophysical properties. They injected different amounts of bone cement with various melting points into the bone cavities and then measured the temperature of the bone-cement interface together with the peripheral bone tissue by using thermocouples to evaluate the potential thermal necrosis. Besides, a 3D human knee model was constructed to assist in evaluating the thermal parameters numerically (Fig. 10e). The data indicated that not only did the larger amount of bone cement cause a higher latent heat, but the higher melting point of LM alloy also resulted in the peak temperature soaring. Moreover, the LM bone cement with higher latent heat had an extended solidification period, causing irreversible damage to the bone tissue.

In conclusion, LM-based cement has good biocompatibility, low melting point, and can be introduced into bodies easily[128]. However, the high latent heat associated with LMs requires more time for solidification and may lead to an irreversible impairment of the surrounding tissues[175]. In general, the LM with a higher melting point (Fig. 10f), higher diameter (Fig. 10g), or a larger amount (Fig. 10h) generates a higher temperament in bone tissues. Therefore, various orthopedic diseases could be treated with different strategies. For example, the LMs with a higher melting point could serve as bone tumor treatment devices, while the lower melting point LMs can be used to treat bone defects. Nonetheless, deeper investigations are required to unveil the miracle of LM bone cements.

E-vessels

Despite the advancements in medical technologies, cardiovascular disease continues to pose a threat to individuals' health. Coronary artery bypass grafting surgery is one of the main treatments to cure the disease.

For instance, Quint et al.[176] introduced an arterial tissue engineering method to fabricate short-term-transplantation tissue-engineered vessels (TEVs). The results indicated that the endothelial progenitor cells and endothelial cells planted in TEVs did not show a tendency for graft occlusion. Besides, another research reported a TEV that shared a similar burst strength with human vessels (>2000 mmHg)[177]. However, lots of the tissue engineering blood vessels (TEBVs), which are fabricated by conventional methods and materials like polyvinyl alcohol-silica ($PVA\text{-}SiO_2$)[178], merely function as stents, and hardly help the new blood vessels to regenerate[176,179–181]. Besides, the complex interactions between the TEBV and blood might induce inflammations, leading to other issues like thrombosis or neointimal hyperplasia[180,182]. Fortunately, Jiang et al.[183]

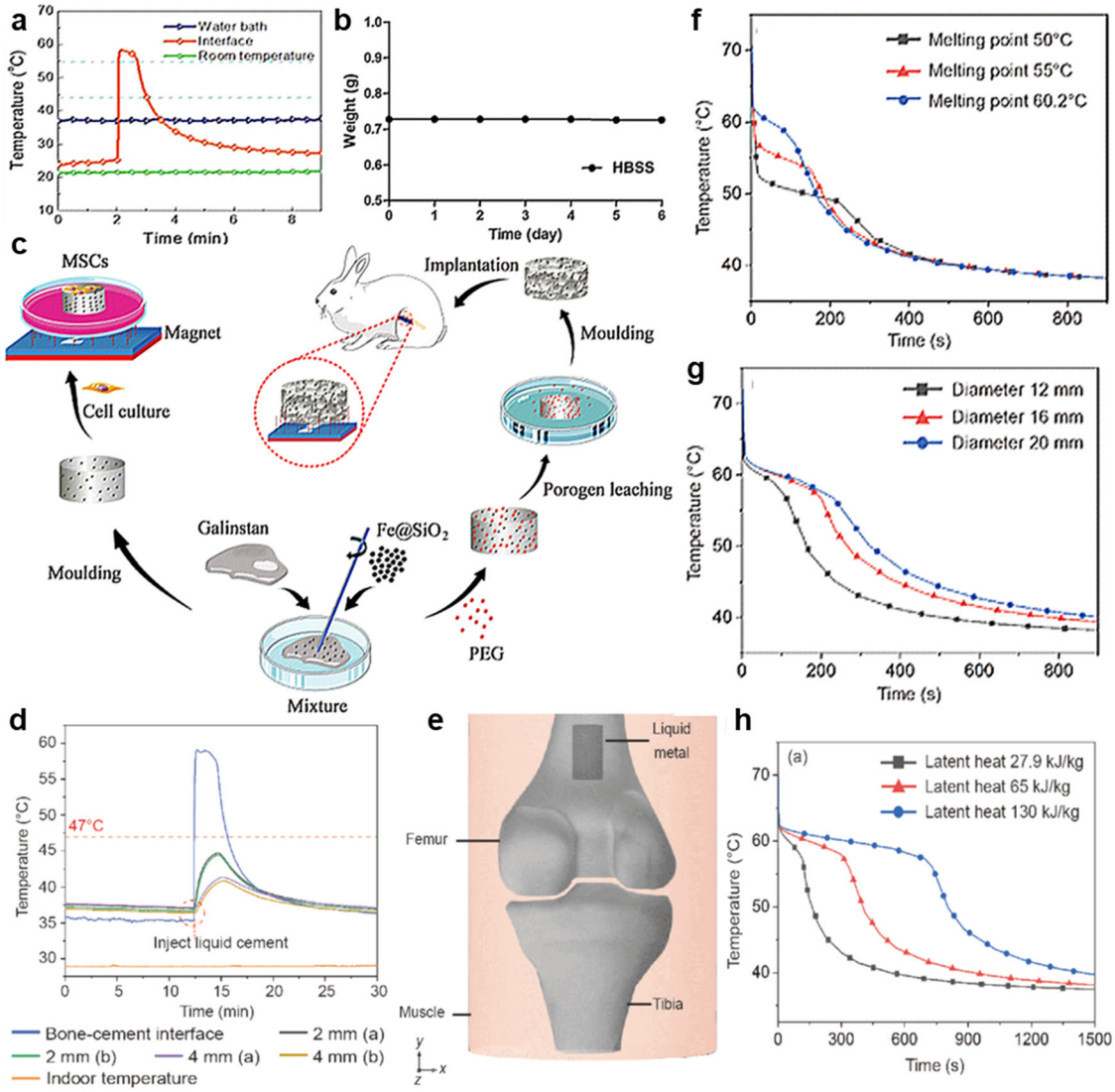

Fig. 10 | LM-based bone cement for bone repairment. a The temperature-time curve of the cement injecting process[129]. Copyright 2014, Elsevier. **b** Mass change of Bi alloy immersed in HBSS solution[128]. Copyright 2021, John Wiley and Sons. **c** The sketch map of the fabrication process[74]. Copyright 2022, Elsevier. **d** The temperature change produced by the liquid-solid phase transition of the LM-based bone cement[175]. **e** The 3D numerical knee model for the temperature simulation[175]. **f–h** The temperature distribution of diverse melting point/volume/amount successively[175]. **d–h** Copyright 2019, Springer Nature.

introduced a kind of TEBV, which was conductive, stretchable and biocompatible, meeting the requirements of clinical surgeries.

The e-vessel (Fig. 11a) was manufactured by rolling up a poly(L-lactide-co-ε-caprolactone) (PLC) based MPC membrane (Fig. 11b) with the assistance of a polytetrafluorethylene mandrel. The MPC had a conductivity of about 8 × 103 S cm^{-1}, and its resistance remained stable, even after being bent and rubbed approximately 1000 times. This remarkable conductivity of the MPC enables the e-vessel to hold a promising application in monitoring and treating diseased regions. Moreover, in-situ monitoring and in vivo implantation in rabbits demonstrated good biocompatibility and stability of the e-vessel. Figure 11c illustrates the diameter of the e-vessel during the implantation, while Fig. 11d shows the velocity distribution of blood flow at the e-vessels from numerous rabbits (Fig. 11e, f) at different time points. Both of which indicated the marvelous biocompatibility of the e-vessel. Furthermore, the e-vessel also performs marvelously in mechanical testing (Fig. 12a–f) and in vivo (Fig. 12g). MPC has a much greater elastic modulus (130 MPa) and maximum tensile strength (27 MPa) than the native vessels. Though the compliance of MPC is lower than the native vessels, MPC shares a similar burst pressure (about 2800 mmHg) with the native carotid artery. Generally, the robust mechanical properties like maximum elongation, elastic modulus, and maximum tensile strength guarantee the MPC a potentially competent in replacing the pathological vessel.

In summary, the electron vessel shows the promise in treating cardiovascular disorders. In the future, by combining the e-vessel with other stretchable electronics, such as sensors, the multifunctional electron vessels could serve as replacements for the original vessels and enable the monitoring and treatment of cardiovascular disease. Nonetheless, further research and in vivo testing still hold immense importance before widespread application can be realized.

Heater

Moderate calefaction on the skin can accelerate blood circulation, thus relieving the pain and the cramp[184]. Thermotherapy is a highly effective clinical therapy for a wide range of diseases, known for its low side effects. However, traditional heaters often face challenges when maintaining their heating temperature during stretching or movement, reducing their functionality[185]. For example, the resistance of conventional conductive fibers changes significantly after stretching, which may result in the uncontrollability of temperature when using heaters, leading to inconvenience and even hurt[186]. On the other hand, although the addition of

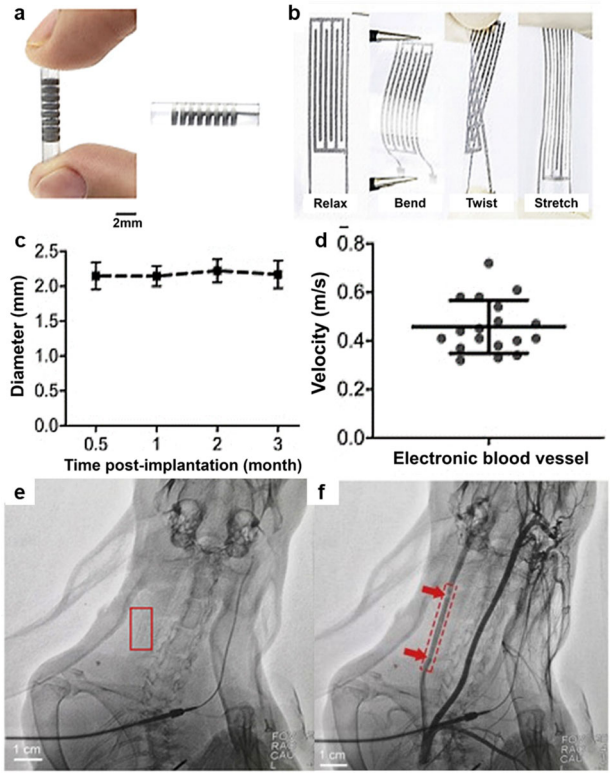

Fig. 11 | LM-based e-vessels in tissue treatment. a Photographs of the electronic blood vessel[183]. **b** Photographs of the MPC-PLC membrane[183]. **c** The diameter changes in the electronic blood vessel after different times post-implantation. The error bars show the standard deviation[183]. **d** The scatter diagram of the velocity of blood flow at the operational site, where the middle velocity was about 0.47 m·s^{-1}. The error bars show the standard deviation[183]. **e**, **f** Image before injecting the contrast medium. The red box indicates the position of the implanted electronic blood vessel. The scale bar is 1 cm[183]. **a**–**f** Copyright 2020, Elsevier.

conductive particles can stabilize the stretching conductivity of the conductive fibers, it also increases the stiffness of the conductive fibers[187]. In contrast, LM-based heaters provide an ingenious solution[97,188–190].

Wang et al.[185], proposed a stretchable LM-based heater that showcases the immense potential of LM in wearable thermotherapy devices. The heater is made of Ga-based LM and polydimethylsiloxane (PDMS). The LM@PDMS heater demonstrated outstanding conductivity (1.81×10^3 S cm^{-1}) and stretchability (over 100% strain). Figure 13a illustrates the relationship between saturation temperature and stretching strain under 2.0 V for heating 240 s, and the decay of saturation temperature is less than 8%. Moreover, Wang and the team captured photos of the heaters during various exercise states, accompanied by corresponding infrared thermal images (Fig. 13b), thus illustrating the heater's ability to maintain a stable heating temperature during physical activity. Furthermore, owing to its high stretchability and simple fabrication procedures, the LM@PDMS heater can be easily molded into various shapes to ensure compatibility with different parts of the body.

Another LM-based heater was introduced in 2022. Tan et al.[189] proposed a strategy for manufacturing liquid metal/carbon nanotube@Ecoflex (LCEF) coaxial conductive filaments. As shown in Fig. 14a–g, the LCEF textiles showed excellent electro-thermal performance under diverse voltages, which indicated the LCEF fabrics have a promising application in wearable heaters.

Besides, there are multitudes of potential applications for LM-based heaters, such as wireless heater-based thermotherapy platforms[188], electronic tattoos[97], and the LM-filled magnetorheological elastomer[190]. Nonetheless, the LM heaters still cannot adjust the temperature automatically with the tissue temperature changing, which might lead to potential scald. Therefore, more research is significantly required to cope with this issue.

Applications oriented towards the human function augmenting

Exoskeleton device and artificial muscle

Exoskeleton devices have the potential to assist elderly and disabled patients in movement, increase human strength, and seize human's sights. Scientists have already proposed designs for such devices[191]. With the soar of technology, plentiful novel materials are being explored for exoskeleton devices, and LM is considered as a potential material in this field[192]. The artificial joint is a key focus in the exoskeleton and human function augmenting, and in 2010, scientists developed a smart hydraulic joint for robotic structures[193], making the manufacturing of artificial joints for mankind a promising endeavor[194].

For instance, Liu et al.[195] reported a flexible mechanical exoskeleton (Fig. 15a) with a low melting point and easily underwent liquid-solid phase transition. This exoskeleton had two working states. When the wearer needed to carry loads, the LM-based exoskeleton was cooled into a solid state with the assistance of the cooling device, which then supported the arm handling the loads. On the contrary, the exoskeleton would be heated into a liquid state after working to improve the comfort level. The mechanical test, compared with the paraffin phase change material (Fig. 15b), demonstrated the extraordinary mechanical strength of the LM-based exoskeleton.

Similarly, the LM-based exoskeleton can also be applied to artificial muscles. Shu et al.[196] proposed a liquid metal artificial muscle (LMAM) that could work in various solutions with a pH range from 0 to 14. The LMAM had a maximum expanding speed of 15 mm s^{-1} and generated actuation strains of up to 87%. Moreover, the low driving voltage (0.5 V) indicated that a small energy supply system satisfied the need for LMAM. Furthermore, LM consisted of the actuating component, averting mechanical fatigue and movement limitation. Not only could the LMAM mimic the tail fin of the fish, but it also had a promising future in biomedical devices.

The intrinsic fluidity and the electrical conductivity of Ga-based liquid metal (GbLM) enable the GbLM to play an irreplaceable role in stretchable electron devices. A method of manufacturing the high-aspect-ratio LM was presented in 2022, and the high-aspect-ratio LM pattern could be applied to the area of wearable flexible devices, orienting towards human function augmenting and therapy[197].

E-skin

Electronic skins have also attracted wide scientific interest. One of the most important functions of e-skins is monitoring human health. Several e-skin monitors have been proposed in recent years by researchers[198,199], and LMs have already been regarded as a potential material for e-skins[200,201].

For instance, Gao et al.[202] proposed an LM-based electronic skin based on embedded Galinstan microchannels and could distinguish the pressure variation less than 50 Pa under the initial pressure of fewer than 100 Pa within 90 ms. Another research reported a wearable touch sensor that could operate from 4 kPa to 100 kPa with a high sensitivity of 0.05 kPa^{-1} [203]. The e-skins not only served as sensors, but they could also be used for temperature-conditioned devices[204]. In 2021, Xiang et al.[205] introduced a self-powered LM-based electronic skin, which helped with thermoregulation. The team adjusted the proportion of Ga, In, and Sn to modify the melting point of the alloy, so that thermoregulating electronic skin (TE-skin) could transform its phase according to the surrounding temperature. As shown in Fig. 15c, the temperature of TE-skin kept stable at around 30 °C when melted, which was a comfortable temperature for human skin[206]. Moreover, LM-based electronic skins could also be utilized as anti-microbial screens and other electronic devices (Fig. 15d–g). Xu et al.[207] proposed an EGaIn-based soft conductor with high anti-leakage and anti-microbial characteristics. The experiment showed that the soft conductor could inactivate more than 97% of the SARS-CoV-2 virus in 10 s. Thus, it could serve as a long-term biomedical electronic skin.

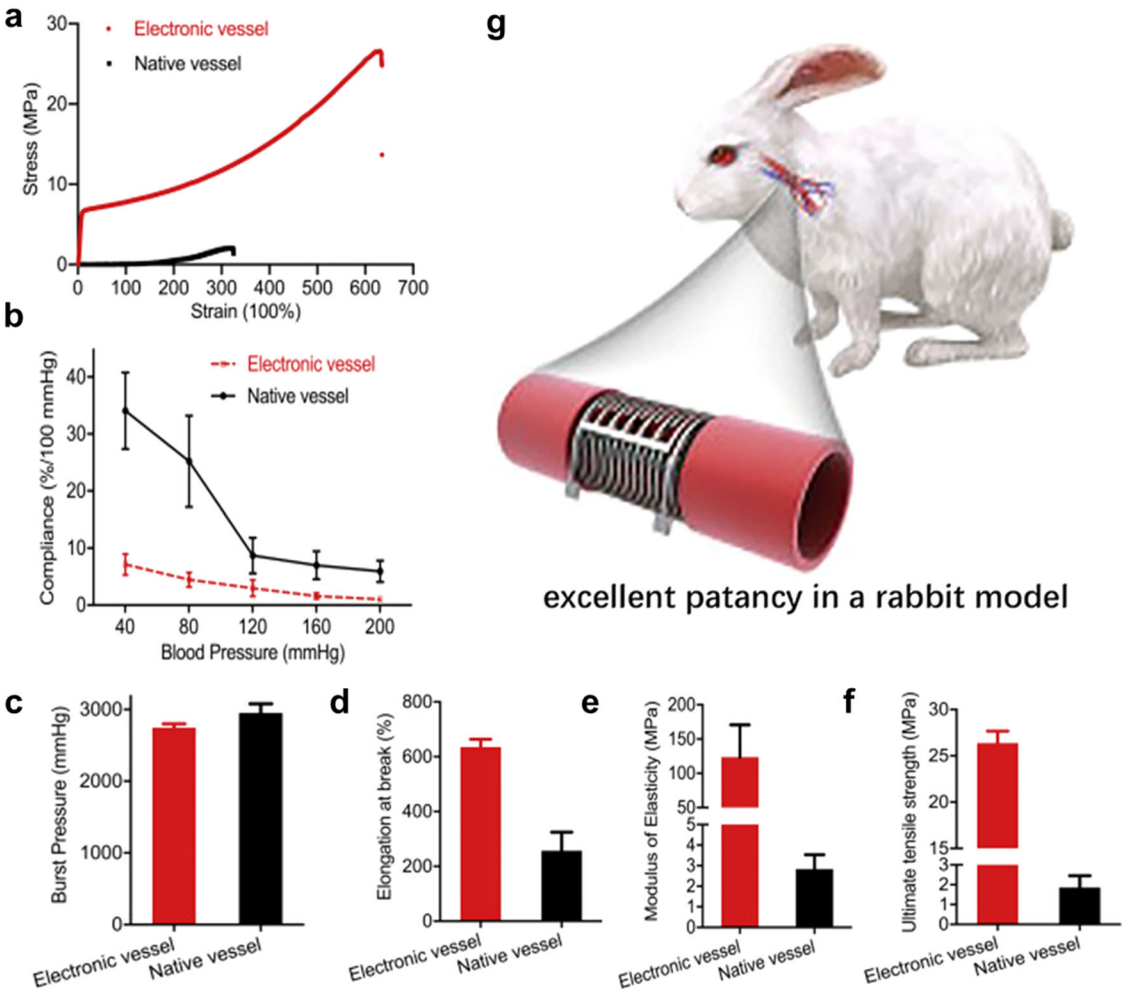

Fig. 12 | The different behaviors between e-vessels and native vessels. a The curve of stress-strain comparison between the electronic vessel and native vessel[183]. **b** The compliance test comparison between the electronic vessel and the native vessel[183]. **c** The burst pressure test comparison between the electronic vessel and the native vessel[183]. **d** The elongation at break comparison between the electronic vessel and native vessel[183]. **e** The modulus of elasticity comparison between the electronic vessel and the native vessel[183]. **f** The ultimate tensile strength comparison between the electronic vessel and the native vessel[183]. **b**–**f** The error bars show the standard deviation. **g** A schematic of the e-vessel of the rabbit[183]. **a**–**g** Copyright 2020, Elsevier.

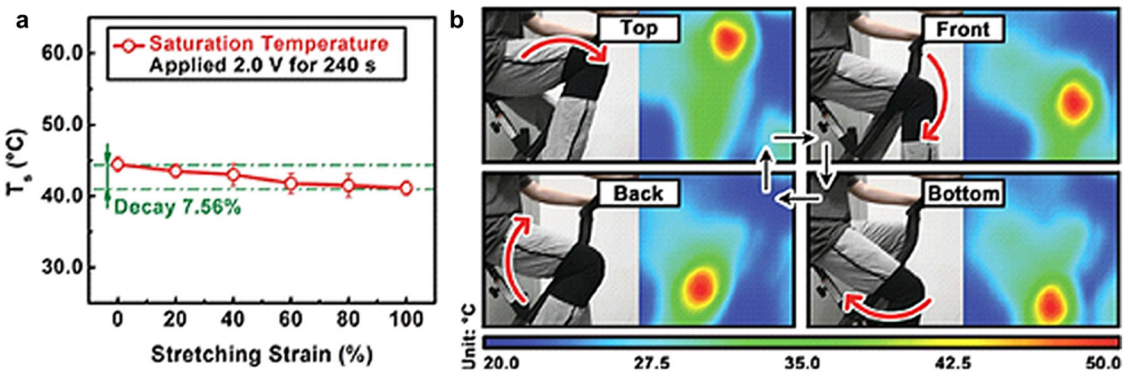

Fig. 13 | Electrical and thermal behavior tests of LM-based heaters. a The strain-temperature diagram of the stretchable LM-heater under 2.0 V for heating 240 s. The error bars show the standard deviation[185]. **b** Photographs and IR thermal images of exercise at different states[185]. **a**, **b** Copyright 2018, John Wiley and Sons.

Challenges and prospects

Equipped with properties such as good biocompatibility[29–34], electrical conductivity[36,46], and stretchability[37], LMs are promising materials for biomedical devices. Nevertheless, several challenges must be addressed before their widespread use.

First and foremost, the corrosion of LMs in a biological environment is an issue that needs to be solved. Many LMs are susceptible to corrosion in the presence of moisture[208], which can damage LM-based devices and impair their performance. Additionally, LMs are highly reactive and can release ions[60], potentially causing harm to local tissue if they react with

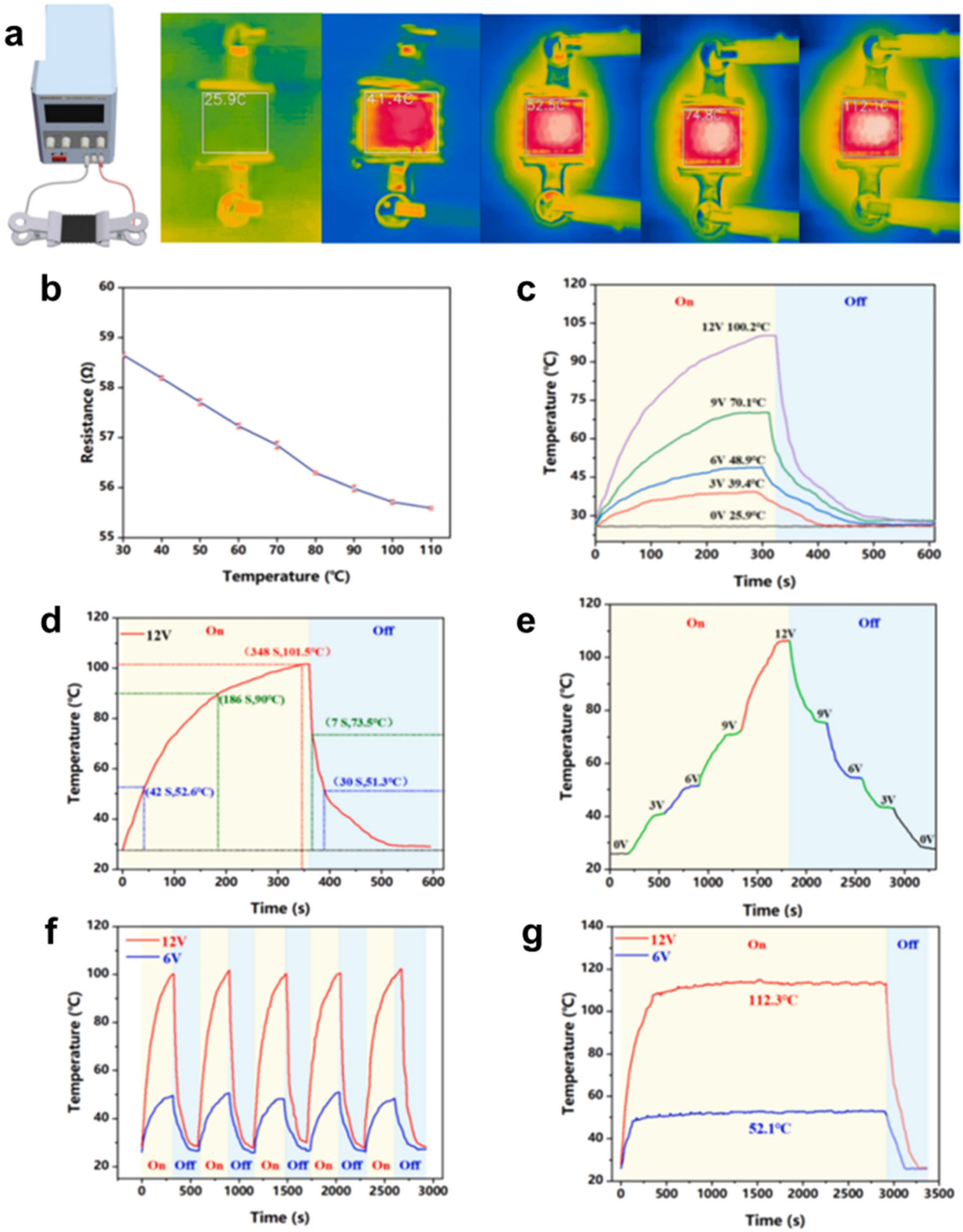

Fig. 14 | Electro-thermal performance of LCEF fabrics. **a** Infrared images of the woven fabric at different voltages[189]. **b** The temperature sensing result of the LCEF is from 30 °C to 110 °C. The error bars show the standard deviation[189]. **c** The heating results of the woven fabric at different voltages[189]. **d** The heating results of the woven fabric at 12 V[189]. **e** Stepped heating results of the woven fabric at different voltages[189]. **f** Heating cyclic test results of the woven fabric at 6 V and 12 V[189]. **g** Long-term heating stability test of the woven fabric at 6 V and 12 V[189]. **a**–**g** Copyright 2023, Elsevier.

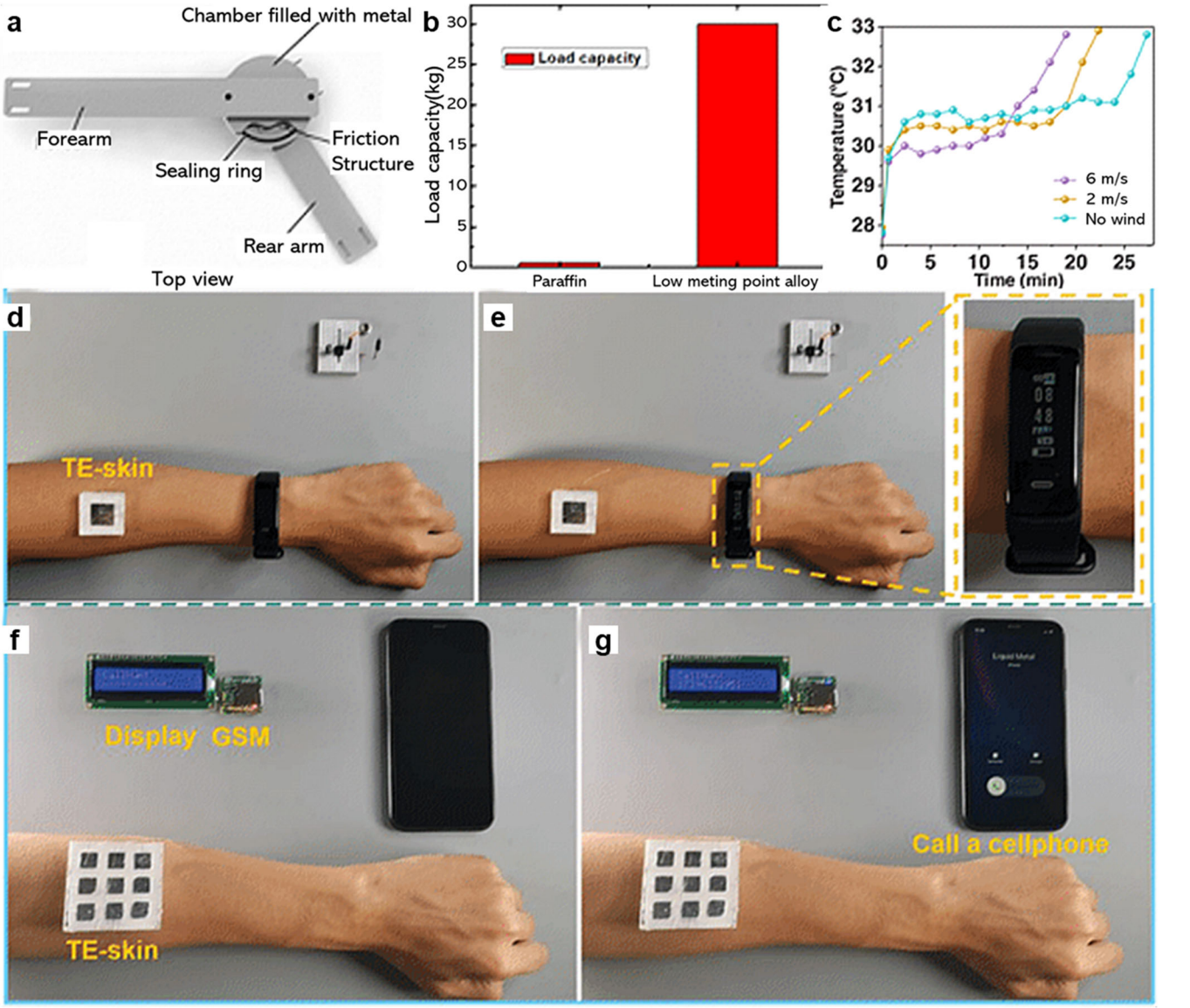

Fig. 15 | LM-based exoskeleton devices and e-skins. a The top view of the flexible mechanical exoskeleton[195]. **b** Comparison of mechanical strength between conventional paraffin-based mechanical joints and that based on low melting point alloy[195]. **a**, **b** Copyright 2014, American Society of Mechanical Engineers. **c** The temperature changes of TE-skin under various airflows, where the temperature of the film heater is 40 °C[205]. **d**, **e** A bracket was charged by TE-skin on the human arm[205]. **f**, **g** A cellphone was dialed by the TE-skin[205]. **c**–**g** Copyright 2024, John Wiley and Sons.

human organs[133]. Moreover, there is still a lack of long-term biosafety experiments and clinical practice, limiting the clinical results[60,209]. Another challenge is the high cost of LMs compared to other materials used in biomedical devices[210]. Furthermore, the fabrication of LM-based biomedical devices requires specialized equipment[164], adding to the manufacturing costs. Additionally, LMs are not ideal for fabricating disposable electronic devices[211]. The stability of LM-based devices is also a significant issue that needs to be addressed. The active nature of Ga, Bi, In, and Sn atoms can result in incorrect connections under electric fields[209]. Besides, the connection between rigid electron devices and the LM circuit is unstable, leading to the inhomogeneous current distribution and accelerating the failure of LM-based devices.

LMs also show their marvelous effect in other biomedical fields. For instance, LMs can serve as raw materials for fabricating nano-targeted medicine for cancer treatment[212]. However, as a relatively new material, LMs require deeper investigation before being applied to biomedical devices. Further research is needed to optimize the application of LMs in biomedical devices, such as modifying LM-based nano-targeted medicine using proteins[213]. Despite these challenges, the prospects for LMs in biomedical devices remain promising. With continued research and development, more effective, efficient, economical, and easily processed facilities can be developed. LM-based biomedical devices can revolutionize medical technology.

Conclusions

As biocompatible, electrical, and thermally conductive, stretchable, and chemically stable materials, LMs exhibit promising prospects in biomedical applications. LMs can serve as neural interfaces, alloy cements, e-vessels, and heaters, facilitating disease treatment and improving human health. LMs also hold great potential for human function augmenting, such as exoskeletons and e-skins. Nevertheless, there are challenges to address in the biomedical use of LMs, including high costs and corrosive issues. With deeper investigations and further development of LMs, the revolution of medical technology can be realized, satisfying the public's demand for an enhanced quality of life.

Data availability

The graphical data and other findings in this paper are available from the corresponding author upon reasonable request.

Code availability

All custom codes regarded as central to the conclusions are available from the corresponding authors upon reasonable request.

Received: 24 September 2023; Accepted: 4 February 2024;
Published online: 20 February 2024

References

1. Mehrotra, P. Biosensors and their applications – A review. *J. Oral. Biosci.* **6**, 153–159 (2016).
2. Haleem, A., Javaid, M., Singh, R. P., Suman, R. & Rab, S. Biosensors applications in medical field: a brief review. *Sens. Int.* **2**, 100100 (2021).
3. Zhu, J. et al. Modified poly(methyl methacrylate) bone cement in the treatment of Kümmell disease. *Regen. Biomater.* **8**, rbaa051 (2021).
4. Sophocleous, M. & Atkinson, J. K. A review of screen-printed silver/silver chloride (Ag/AgCl) reference electrodes potentially suitable for environmental potentiometric sensors. *Sens. Actuators A Phys.* **267**, 106–120 (2017).
5. Tao, Z. et al. Facile oxidation of superaligned carbon nanotube films for primary cell culture and genetic engineering. *J. Mater. Chem. B* **2**, 471–476 (2014).
6. Bong, J. et al. Radiolucent implantable electrocardiographic monitoring device based on graphene. *Carbon* **152**, 946–953 (2019).
7. Zhu, J. et al. Laser-induced graphene non-enzymatic glucose sensors for on-body measurements. *Biosens. Bioelectron.* **193**, 113606 (2021).
8. Lim, S. H., Wei, J., Lin, J., Li, Q. & KuaYou, J. A glucose biosensor based on electrodeposition of palladium nanoparticles and glucose oxidase onto Nafion-solubilized carbon nanotube electrode. *Biosens. Bioelectron.* **20**, 2341–2346 (2005).
9. Zhang, J. et al. Construction of titanium dioxide nanorod/graphite microfiber hybrid electrodes for high performance electrochemical glucose biosensor. *Nanoscale* **8**, 9382–9389 (2016).
10. Huang, H. et al. Construction of flexible enzymatic electrode based on gradient hollow fiber membrane and multi-wall carbon tubes meshes. *Biosens. Bioelectron.* **152**, 112001 (2020).
11. Castagnola, E. et al. PEDOT-CNT-coated low-impedance, ultra-flexible, and brain-conformable Micro-ECoG arrays. *IEEE Trans. Neural Syst. Rehabil. Eng.* **23**, 342–350 (2015).
12. Guernion, N. J. L. & Hayes, W. 3- and 3,4-Substituted Pyrroles and thiophenes and their corresponding polymers - a review. *Curr. Org. Chem.* **8**, 637–651 (2004).
13. Kang, S.-K. et al. Bioresorbable silicon electronic sensors for the brain. *Nature* **530**, 71–76 (2016).
14. Gao, W. & Yu, C. Wearable and implantable devices for healthcare.*Adv. Healthcare Mater.* **10**, 2101548 (2021).
15. Li, Y. W. et al. A novel injectable bioactive bone cement for spinal surgery: a developmental and preclinical study. *J. Biomed. Mater. Res.* **52**, 164–170 (2000).
16. Xu, H. H. K. et al. Calcium phosphate cements for bone engineering and their biological properties. *Bone Res.* **5**, 1–19 (2017).
17. Yang, J.-M. Polymerization of acrylic bone cement using differential scanning calorimetry. *Biomaterials* **18**, 1293–1298 (1997).
18. Bu, F., Li, C., Wang, Q. & Liu, X. Ultraviolet-assisted printing of flexible all-solid-state zinc batteries with enhanced interfacial bond. *Chem. Eng. J.* **449**, 137710 (2022).
19. ToolBox, E. *Young's Modulus, Tensile Strength and Yield Strength Values for some Materials*. https://www.engineeringtoolbox.com/young-modulus-d_417.html (2023.4.6).
20. Arash, B., Wang, Q. & Varadan, V. K. Mechanical properties of carbon nanotube/polymer composites. *Sci. Rep.* **4**, 6479 (2014).
21. Murjani, B. O., Kadu, P. S., Bansod, M., Vaidya, S. S. & Yadav, M. D. Carbon nanotubes in biomedical applications: current status, promises, and challenges. *Carbon Lett.* **32**, 1207–1226 (2022).
22. Alshehri, R. et al. Carbon nanotubes in biomedical applications: factors mechanisms, remedies toxic.*J. Med. Chem.* **59**, 8149–8167 (2016).
23. Namsheer, K. & Rout, C. S. Conducting polymers: a comprehensive review on recent advances in synthesis, properties and applications. *RSC Adv.* **11**, 5659–5697 (2021).
24. Zhang, N., Xiong, G. & Liu, Z. Toxicity of metal-based nanoparticles: challenges in the nano era. *Front. Bioeng. Biotechnol.* **10**, 1001572 (2022).
25. Yang, L. et al. Toxicity of mercury: molecular evidence. *Chemosphere* **245**, 125586 (2020).
26. Mason, P. E. et al. Coulomb explosion during the early stages of the reaction of alkali metals with water. *Nat. Chem.* **7**, 250–254 (2015).
27. Jolly, W. L. Advances in inorganic chemistry and radiochemistry, Vol 5 (eds. H. J. Emeléus and A. G. Sharpe) 1319–1320, (Elsevier, 1964).
28. Cochran, C. N. & Foster, L. M. Vapor pressure of gallium, stability of gallium suboxide vapor, and equilibria of some reactions producing Gallium Suboxide Vapour.*J. Electrochem. Soc.* **109**, 144–148 (1962).
29. Milheiro, A. et al. In vitro cytotoxicity of metallic ions released from dental alloys. *Odontology* **104**, 136–142 (2016).
30. Psarras, V., Wennberg, A. & Dérand, T. Cytotoxicity of corroded gallium and dental amalgam alloys. An in vitro study. *Acta Odontol. Scand.* **50**, 31–36 (1992).
31. Shaini, F. J., Shelton, R. M., Marquis, P. M. & Shortall, A. C. In vitro evaluation of the effect of freshly mixed amalgam and gallium-based alloy on the viability of primary periosteal and osteoblast cell cultures. *Biomaterials* **21**, 113–119 (2000).
32. Hou, F., Zhang, J., Sun, X. & Sheng, L. Study on the biocompatibility of Ga-based and Al-assisted self-driven liquid metal in cell and animal experiments for drug delivery. *Biomed. Mater. Eng.* **32**, 229–242 (2021).
33. Sevcikova, J. & Pavkova Goldbergova, M. Biocompatibility of NiTi alloys in the cell behaviour. *BioMetals* **30**, 163–169 (2017).
34. Foremny, K., Nagels, S., Kreienmeyer, M., Doll, T. & Deferme, W. Biocompatibility testing of liquid metal as an interconnection material for flexible implant technology. *Nanomaterials* **11**, 3251 (2021).
35. Mou, L. et al. Highly stretchable and biocompatible liquid metal-elastomer conductors for self-healing electronics. *Small* **16**, 2005336 (2020).
36. Ning, N. et al. Highly stretchable liquid metal/polyurethane sponge conductors with excellent electrical conductivity stability and good mechanical properties. *Compos. B Eng.* **179**, 107492 (2019).
37. Liu, S. et al. Fabrication of liquid metal loaded polycaprolactone conductive film for biocompatible and flexible electronics. *Biosens. Bioelectron. X* **11**, 100182 (2022).
38. Hiran, C. et al. Liquid metal incorporated graphene oxide films with enhanced through-plane thermal conductivity and flame resistance. *Appl. Mater. Today* **29**, 101617 (2022).
39. Moon, S. et al. 3D Printable concentrated liquid metal composite with high thermal conductivity. *iScience* **24**, 103183 (2021).
40. Kong, W. et al. High thermal conductivity in multiphase liquid metal and silicon carbide soft composites. *Adv. Mater. Interfaces* **8**, 2100069 (2021).
41. Krings, E. J. et al. Lightweight, thermally conductive liquid metal elastomer composite with independently controllable thermal conductivity and density. *Small* **17**, 2104762 (2021).
42. Jung, J., Jeong, S. H., Hjort, K. & Ryu, S. Investigation of thermal conductivity for liquid metal composites using the micromechanics-

based mean-field homogenization theory. *Soft Matter* **16**, 5840–5847 (2020).
43. Sargolzaeiaval, Y. et al. High thermal conductivity silicone elastomer doped with graphene nanoplatelets and eutectic gain liquid metal alloy. *ECS J. Solid State Sci. Technol.* **8**, 357 (2019).
44. Viswanath, D. S. & Mathur, B. C. Thermal conductivity of liquid metals and alloys. *Metall. Mater. Trans. B* **3**, 1769–1772 (1972).
45. Powell, R. W. Bidwell's intercept relation and the thermal conductivity of liquid metals. *J. Appl. Phys.* **19**, 995–996 (1948).
46. Houshyar, S. et al. Liquid metal polymer composite: flexible, conductive, biocompatible, and antimicrobial scaffold. *J. Biomed. Mater. Res. B Appl. Biomater.* **110**, 1131–1139 (2021).
47. Ye, J., Xing, Z.-R., Gao, J.-Y. & Liu, J. Liquid metal coil. *Mater. Today Commun.* **32**, 104120 (2022).
48. Rahman, M. A., Shiroma, W. A. & Ohta, A. T. Liquid-metal capacitors with a 42:1 tuning ratio. *Electron. Lett.* **53**, 710–711 (2017).
49. Fassler, A. & Majidi, C. Soft-matter capacitors and inductors for hyperelastic strain sensing and stretchable electronics. *Smart Mater. Struct.* **22**, 055023 (2013).
50. Lazarus, N., Meyer, C., Bedair, S., Nochetto, H. & Kierzewski, I. Multilayer liquid metal stretchable inductors. *Smart Mater. Struct.* **23**, 085036 (2014).
51. Guo, S. et al. Flexible liquid metal coil prepared for electromagnetic energy harvesting and wireless charging. *Front. Energy* **13**, 474–482 (2019).
52. Koo, H. J., So, J. H., Dickey, M. D. & Velev, O. D. Towards all-soft matter circuits: prototypes of quasi-liquid devices with memristor characteristics. *Adv. Mater.* **23**, 3559–3564 (2011).
53. Zaheer, M. et al. Liquid-metal-induced memristor behavior in polymer insulators. *Phys. Status Solidi Rapid Res. Lett.* **14**, 2000050 (2020).
54. Zaheer, M. et al. All solution-processed inorganic, multilevel memristors utilizing liquid metals electrodes suitable for analog computing. *ACS Omega* **7**, 40911–40919 (2022).
55. Guo, X. et al. Doped 2D SnS materials derived from liquid metal-solution for tunable optoelectronic devices. *Nanoscale* **14**, 6802–6810 (2022).
56. Kozaki, T. et al. Liquid-state optoelectronics using liquid metal. *Adv. Electron. Mater.* **6**, 1901135 (2020).
57. Alsaif, M. M. et al. 2D SnO/In2O3 van der Waals heterostructure photodetector based on printed oxide skin of liquid metals. *Adv. Mater. Interfaces* **6**, 1900007 (2019).
58. Kim, D. et al. Effective delivery of anti-cancer drug molecules with shape transforming liquid metal particles. *Cancers* **11**, 1666 (2019).
59. Liu, H. et al. Novel contrast media based on the liquid metal gallium for in vivo digestive tract radiography: a feasibility study. *BioMetals* **32**, 795–801 (2019).
60. Rui, G. & Jing, L. Implantable liquid metal-based flexible neural microelectrode array and its application in recovering animal locomotion functions. *J. Micromech. Microeng.* **27**, 104002 (2017).
61. Pyatin, V. F., Kolsanov, A. V. & Shirolapov, I. V. Recent medical techniques for peripheral nerve repair: nerve guidance conduits update. *Adv. Gerontol.* **29**, 741–750 (2016).
62. Cole, K. J., Daley, B. J. & Brand, R. A. The sensitivity of joint afferents to knee translation. *Sportverletz. Sportschaden* **10**, 27–31 (1996).
63. Xu, S., Zong, Y., Ma, J. & Liu, L. A multifunctional skin-like sensor based on liquid metal activated gelatin organohydrogel. *Adv. Mater. Interfaces* **9**, 2201212 (2022).
64. Md Saifur, R., Julia, E. H., Andrew, B. H. & William, J. S. Broadband mechanoresponsive liquid metal sensors. *npj Flex. Electron.* **6**, 71 (2022).
65. Zhang, R. et al. Liquid metal electrode-enabled flexible microdroplet sensor. *Lab Chip* **20**, 496–504 (2019).
66. Xiaoping, Z., Yi, H. & Jie, Z. Liquid metal antenna-based pressure sensor. *Smart Mater. Struct.* **28**, 025019 (2019).
67. Varga, M., Ladd, C., Ma, S., Holbery, J. & Tröster, G. On-skin liquid metal inertial sensor. *Lab Chip* **17**, 3272–3278 (2017).
68. Choe, M. et al. Ultrasoft and ultrastretchable wearable strain sensors with anisotropic conductivity enabled by liquid metal fillers. *Micromachines* **14**, 17 (2023).
69. Gao, W., Wang, Y., Wang, Q., Ma, G. & Liu, J. Liquid metal biomaterials for biomedical imaging. *J. Mater. Chem. B* **10**, 829–842 (2022).
70. Yan, J., Lu, Y., Chen, G., Yang, M. & Gu, Z. Advances in liquid metals for biomedical applications. *Chem. Soc. Rev.* **47**, 2518–2533 (2018).
71. Yang, X. et al. Recent development and advances on fabrication and biomedical applications of Ga-based liquid metal micro/nanoparticles. *Compos. B. Eng.* **248**, 110384 (2023).
72. Yang, N., Gong, F., Zhou, Y., Yu, Q. & Cheng, L. Liquid metals: Preparation, surface engineering, and biomedical applications. *Coord. Chem. Rev.* **471**, 214731 (2022).
73. Hallfors, N., Khan, A. I., Dickey, M. D. & Taylor, A. M. Integration of pre-aligned liquid metal electrodes for neural stimulation within a user-friendly microfluidic platform. *Lab Chip* **13**, 522–526 (2013).
74. Li, S., Dong, C. & Lv, Y. Magnetic liquid metal scaffold with dynamically tunable stiffness for bone tissue engineering. *Biomater. Adv.* **139**, 212975 (2022).
75. Zavabeti, A. et al. A liquid metal reaction environment for the room-temperature synthesis of atomically thin metal oxides. *Science* **358**, 332–335 (2017).
76. Blaiszik, B. J. et al. Autonomic restoration of electrical conductivity. *Adv. Mater.* **24**, 398–401 (2012).
77. Tang, J. et al. Gallium-based liquid metal amalgams: transitional-state metallic mixtures (TransM2ixes) with enhanced and tunable electrical, thermal, and mechanical properties. *ACS Appl. Mater. Interfaces* **9**, 35977–35987 (2017).
78. Kong, W. et al. Oxide-mediated formation of chemically stable tungsten–liquid metal mixtures for enhanced thermal interfaces. *Adv. Mater.* **31**, 1904309 (2019).
79. Li, J. et al. Analytical and experimental studies of the improved conductance-stability and stretchability of the liquid metal-embedded composites based on novel continuous annular-shaped branch channels. *J. Mater. Res. Technol.* **26**, 9315–9327 (2023).
80. Li, W. et al. Microfluidic fabrication of microparticles for biomedical applications. *Chem. Soc. Rev.* **47**, 5646–5683 (2018).
81. Lopes, P. A., Paisana, H., De Almeida, A. T., Majidi, C. & Tavakoli, M. Hydroprinted electronics: ultrathin stretchable Ag–In–Ga E-skin for bioelectronics and human–machine interaction. *ACS Appl. Mater. Interfaces* **10**, 38760–38768 (2018).
82. Lin, P. et al. Capillary-based microfluidic fabrication of liquid metal microspheres toward functional microelectrodes and photothermal medium. *ACS Appl. Mater. Interfaces* **11**, 25295–25305 (2019).
83. Tang, S.-Y. et al. Liquid metal enabled pump. *Proc. Natl. Acad. Sci. USA* **111**, 3304–3309 (2014).
84. Carey, B. J. et al. Wafer-scale two-dimensional semiconductors from printed oxide skin of liquid metals. *Nat. Commun.* **8**, 14482 (2017).
85. David, R. & Miki, N. Tunable noble metal thin films on ga alloys via galvanic replacement. *Langmuir* **34**, 10550–10559 (2018).
86. Zavabeti, A. et al. Green synthesis of low-dimensional aluminum oxide hydroxide and oxide using liquid metal reaction media: ultrahigh flux membranes. *Adv. Funct. Mater.* **28**, 1804057 (2018).
87. Dickey, M. D. Stretchable and soft electronics using liquid metals. *Adv. Mater.* **29**, 1606425 (2017).
88. Majidi, C. Soft robotics: a perspective—current trends and prospects for the future. *Soft Robot.* **1**, 5–11 (2013).
89. Kim, K., Park, Y.-G., Hyun, B. G., Choi, M. & Park, J.-U. Recent advances in transparent electronics with stretchable forms. *Adv. Mater.* **31**, 1804690 (2019).

90. Daeneke, T. et al. Liquid metals: fundamentals and applications in chemistry. *Chem. Soc. Rev.* **47**, 4073–4111 (2018).
91. Zhou, Y. et al. A universal method to produce low–work function electrodes for organic electronics. *Science* **336**, 327–332 (2012).
92. Comiskey, B., Albert, J. D., Yoshizawa, H. & Jacobson, J. An electrophoretic ink for all-printed reflective electronic displays. *Nature* **394**, 253–255 (1998).
93. Minemawari, H. et al. Inkjet printing of single-crystal films. *Nature* **475**, 364–367 (2011).
94. Chen, S. & Liu, J. Pervasive liquid metal printed electronics: From concept incubation to industry. *iScience* **24**, 102026 (2021).
95. Zheng, Y., He, Z., Gao, Y. & Liu, J. Direct desktop printed-circuits-on-paper flexible electronics. *Sci. Rep.* **3**, 1786 (2013).
96. Ren, L., Xu, X., Du, Y., Kalantar-Zadeh, K. & Dou, S. X. Liquid metals and their hybrids as stimulus–responsive smart materials. *Mater. Today* **34**, 92–114 (2020).
97. Guo, R. et al. Semi-Liquid-Metal-(Ni-EGaIn)-based ultraconformable electronic tattoo. *Adv. Mater. Technol.* **4**, 1900183 (2019).
98. Chen, R. et al. Magnetically controllable liquid metal marbles. *Adv. Mater. Interfaces* **6**, 1901057 (2019).
99. Merhebi, S. et al. Magnetic and conductive liquid metal gels. *ACS Appl. Mater. Interfaces* **12**, 20119–20128 (2020).
100. Chen, Y. et al. Robust fabrication of nonstick, noncorrosive, conductive graphene-coated liquid metal droplets for droplet-based, floating electrodes. *Adv. Funct. Mater.* **28**, 1706277 (2018).
101. Guo, Z. et al. Galvanic replacement reaction for in situ fabrication of litchi-shaped heterogeneous liquid metal-Au nano-composite for radio-photothermal cancer therapy. *Bioact. Mater.* **6**, 602–612 (2021).
102. Hoshyargar, F., Crawford, J. & O'Mullane, A. P. Galvanic replacement of the liquid metal galinstan. *J. Am. Chem. Soc.* **139**, 1464–1471 (2017).
103. Xia, N. et al. Multifunctional and flexible ZrO2-coated EGaIn nanoparticles for photothermal therapy. *Nanoscale* **11**, 10183–10189 (2019).
104. Zheng, R.-m et al. A novel conductive core–shell particle based on liquid metal for fabricating real-time self-repairing flexible circuits. *Adv. Funct. Mater.* **30**, 1910524 (2020).
105. Hu, J.-J. et al. Immobilized liquid metal nanoparticles with improved stability and photothermal performance for combinational therapy of tumor. *Biomaterials* **207**, 76–88 (2019).
106. Liu, Y. et al. Water-processable liquid metal nanoparticles by single-step polymer encapsulation. *Nanoscale* **12**, 13731–13741 (2020).
107. Zhang, C. et al. Nucleation and growth of polyaniline nanofibers onto liquid metal nanoparticles. *Chem. Mater.* **32**, 4808–4819 (2020).
108. Yan, J. et al. Solution processable liquid metal nanodroplets by surface-initiated atom transfer radical polymerization. *Nat. Nanotechnol.* **14**, 684–690 (2019).
109. Li, X. et al. Liquid metal droplets wrapped with polysaccharide microgel as biocompatible aqueous ink for flexible conductive devices. *Adv. Funct. Mater.* **28**, 1804197 (2018).
110. Thrasher, C. J., Farrell, Z. J., Morris, N. J., Willey, C. L. & Tabor, C. E. Mechanoresponsive polymerized liquid metal networks. *Adv. Mater.* **31**, 1903864 (2019).
111. Peng, W., Cai, Y., Fanslau, L. & Vana, P. Nanoengineering with RAFT polymers: from nanocomposite design to applications. *Polym. Chem.* **12**, 6198–6229 (2021).
112. Xin, Y., Peng, H., Xu, J. & Zhang, J. Ultrauniform embedded liquid metal in sulfur polymers for recyclable, conductive, and self-healable materials. *Adv. Funct. Mater.* **29**, 1808989 (2019).
113. Sun, H. et al. Cancer-cell-biomimetic nanoparticles for targeted therapy of homotypic tumors. *Adv. Mater.* **28**, 9581–9588 (2016).
114. Xu, D. et al. Enzyme-powered liquid metal nanobots endowed with multiple biomedical functions. *ACS Nano* **15**, 11543–11554 (2021).
115. Zhang, Y., Liu, M.-D., Li, C.-X., Li, B. & Zhang, X.-Z. Tumor cell membrane-coated liquid metal nanovaccine for tumor prevention‡. *Chin. J. Chem.* **38**, 595–600 (2020).
116. Tang, L. et al. Printable metal-polymer conductors for highly stretchable bio-devices. *iScience* **4**, 302–311 (2018).
117. Wang, J. et al. Printable superelastic conductors with extreme stretchability and robust cycling endurance enabled by liquid-metal particles. *Adv. Mater.* **30**, 1706157 (2018).
118. Starodubtsev, Y. N. & Tsepelev, V. S. Analysis of surface tension and viscosity of liquid metals. *Metall. Mater. Trans. B* **52**, 1886–1890 (2021).
119. Starodubtsev, Y. N. & Tsepelev, V. S. Analysis of the kinematic viscosity and self-diffusion of liquid metals at the melting temperature. *High. Temp.* **59**, 192–197 (2021).
120. Hildebrand, J. H. & Lamoreaux, R. H. Viscosity of liquid metals: an interpretation. *Proc. Natl. Acad. Sci. USA* **73**, 988–989 (1976).
121. Wang, H. et al. Liquid metal fibers. *Adv. Fiber Mater.* **4**, 987–1004 (2022).
122. Zhu, H. et al. Fully solution processed liquid metal features as highly conductive and ultrastretchable conductors. *Npj Flex. Electron.* **5**, 25 (2021).
123. Wang, L. & Liu, J. Compatible hybrid 3D printing of metal and nonmetal inks for direct manufacture of end functional devices. *Sci. China Technol. Sci.* **57**, 2089–2095 (2014).
124. Sano, Y. et al. Oral toxicity of bismuth in rat: single and 28-day repeated administration studies. *J. Occup. Health* **47**, 293–298 (2005).
125. Larsen, A., Martiny, N., Stoltenberg, M., Danscher, G. & Rungby, J. Gastrointestinal and systemic uptake of bismuth in mice after oral exposure. *Pharmacol. Toxicol.* **93**, 82–90 (2003).
126. Fowler, B. A., Sullivan, D. W., Sexton, M. J. Chapter 31 - Bismuth in Handbook on the Toxicology of Metals (Fourth Edition) (eds. Nordberg, G. F. Fowler, B. A. Nordberg, M.) 655-666 (Academic Press: San Diego, 2015).
127. Remennik, S., Bartsch, I., Willbold, E., Witte, F. & Shechtman, D. New, fast corroding high ductility Mg–Bi–Ca and Mg–Bi–Si alloys, with no clinically observable gas formation in bone implants. *Mater. Sci. Eng. B* **176**, 1653–1659 (2011).
128. He, Y. et al. Injectable affinity and remote magnetothermal effects of Bi-based alloy for long-term bone defect repair and analgesia. *Adv. Sci.* **8**, 2100719 (2021).
129. Yi, L., Jin, C., Wang, L. & Liu, J. Liquid-solid phase transition alloy as reversible and rapid molding bone cement. *Biomaterials* **35**, 9789–9801 (2014).
130. Wang, X. et al. Printed conformable liquid metal e-skin-enabled spatiotemporally controlled bioelectromagnetics for wireless multisite tumor therapy. *Adv. Funct. Mater.* **29**, 1907063 (2019).
131. Creighton, M. A. et al. Oxidation of Gallium-based liquid metal alloys by water. *Langmuir* **36**, 12933–12941 (2020).
132. Kim, J.-H., Kim, S., So, J.-H., Kim, K. & Koo, H.-J. Cytotoxicity of Gallium–Indium liquid metal in an aqueous environment. *ACS Appl. Mater. Interfaces* **10**, 17448–17454 (2018).
133. Chen, S. et al. Toxicity and biocompatibility of liquid metals. *Adv. Healthcare Mater.* **12**, 2201924 (2022).
134. Fan, L. et al. Injectable and radiopaque liquid metal/Calcium Alginate hydrogels for endovascular embolization and tumor embolotherapy. *Small* **16**, 1903421 (2020).
135. Jin, C. et al. Injectable 3-D fabrication of medical electronics at the target biological tissues. *Sci. Rep.* **3**, 3442 (2013).
136. Houshyar, S. et al. Liquid metal polymer composite: flexible, conductive, biocompatible, and antimicrobial scaffold. *J. Biomed. Mater. Res. B Appl. Biomater.* **110**, 1131–1139 (2022).
137. Avery, R. K. et al. An injectable shear-thinning biomaterial for endovascular embolization. *Sci. Transl. Med.* **8**, 365ra156–365ra156 (2016).

138. Song, H. et al. Ga-based liquid metal micro/nanoparticles: recent advances and applications. *Small* **16**, 1903391 (2020).
139. Narayanasamy, P., Switzer, B. L. & Britigan, B. E. Prolonged-acting, multi-targeting Gallium nanoparticles potently inhibit growth of both HIV and mycobacteria in Co-infected human macrophages. *Sci. Rep.* **5**, 8824 (2015).
140. Lin, Y. et al. Sonication-enabled rapid production of stable liquid metal nanoparticles grafted with poly(1-octadecene-alt-maleic anhydride) in aqueous solutions. *Nanoscale* **10**, 19871–19878 (2018).
141. Yu, H.-S., Liao, W.-T. Gallium: environmental pollution and health effects in encyclopedia of environmental health (ed. Jerome, N.), 829–833 (Elsevier, 2011).
142. Yang, N. & Sun, H. Bismuth: environmental pollution and health effects. *Environ. Health Perspect.* **40**, 414–420 (2011).
143. Mao, Y. et al. Nanocellulose-based reusable liquid metal printed electronics fabricated by evaporation-induced transfer printing. *J. Mater. Sci. Technol.* **61**, 132–137 (2021).
144. Scharmann, F. et al. Viscosity effect on GaInSn studied by XPS. *Surf. Interface Anal.* **36**, 981–985 (2004).
145. Huang, P. & Luan, J. Dispersed GaOOH rods loaded on the surface of ZnBiNbO5 particles with enhanced photocatalytic activity toward enrofloxacin. *RSC Adv.* **9**, 32027–32033 (2019).
146. Bark, H. & Lee, P. S. Surface modification of liquid metal as an effective approach for deformable electronics and energy devices. *Chem. Sci.* **12**, 2760–2777 (2021).
147. Lertanantawong, B., Lertsathitphong, P. & O'Mullane, A. P. Chemical reactivity of Ga-based liquid metals with redox active species and its influence on electrochemical processes. *Electrochem. Commun.* **93**, 15–19 (2018).
148. HerØ, H., Okabe, T. & Wie, H. Corrosion of gallium alloys in vivo. *J. Mater. Sci. Mater. Med.* **8**, 357–360 (1997).
149. Wu, Z. et al. Corrosion behavior investigation of gallium coating on magnesium alloy in simulated body fluid. *J. Mater. Res. Technol.* **27**, 225–236 (2023).
150. Liu, Y., Ji, X. & Liang, J. Rupture stress of liquid metal nanoparticles and their applications in stretchable conductors and dielectrics. *Npj Flex. Electron.* **5**, 11 (2021).
151. Gao, H.-L. et al. Macroscopic free-standing hierarchical 3D architectures assembled from silver nanowires by ice templating. *Angew. Chem. Int. Ed.* **53**, 4561–4566 (2014).
152. Kim, Y. et al. Stretchable nanoparticle conductors with self-organized conductive pathways. *Nature* **500**, 59–63 (2013).
153. Lipomi, D. J. et al. Skin-like pressure and strain sensors based on transparent elastic films of carbon nanotubes. *Nat. Nanotechnol.* **6**, 788–792 (2011).
154. Matsuhisa, N. et al. Printable elastic conductors by in situ formation of silver nanoparticles from silver flakes. *Nat. Mater.* **16**, 834–840 (2017).
155. Sekitani, T. et al. Stretchable active-matrix organic light-emitting diode display using printable elastic conductors. *Nat. Mater.* **8**, 494–499 (2009).
156. Evans, G. R. D. Peripheral nerve injury: a review and approach to tissue engineered constructs. *Anat. Rec.* **263**, 396–404 (2001).
157. Scheib, J. & Höke, A. Advances in peripheral nerve regeneration. *Nat. Rev. Neurol.* **9**, 668–676 (2013).
158. Williams, J. C., Rennaker, R. L. & Kipke, D. R. Long-term neural recording characteristics of wire microelectrode arrays implanted in cerebral cortex. *Brain Res.* **4**, 303–313 (1999).
159. Zhang, J., Sheng, L., Jin, C. & Liu, J. Liquid metal as connecting or functional recovery channel for the transected sciatic nerve. Preprint at https://arxiv.org/abs/1404.5931 (2014).
160. Liu, F., Yu, Y., Yi, L. & Liu, J. Liquid metal as reconnection agent for peripheral nerve injury. *Sci. Bull.* **61**, 939–947 (2016).
161. Tang, R. et al. Towards an artificial peripheral nerve: liquid metal-based fluidic cuff electrodes for long-term nerve stimulation and recording. *Biosens. Bioelectron.* **216**, 114600 (2022).
162. Dong, R. et al. Printed stretchable liquid metal electrode arrays for in vivo neural recording. *Small* **17**, 2006612 (2021).
163. Liu, R. et al. Development of three-dimension microelectrode array for bioelectric measurement using the liquidmetal-micromolding technique. *Appl. Phys. Lett.* **103**, 193701 (2013).
164. Zhang, M. et al. Versatile fabrication of liquid metal nano-ink based flexible electronic devices. *Appl. Mater. Today* **22**, 100903 (2021).
165. Lee, M., Shim, H. J., Choi, C. & Kim, D.-H. Soft high-resolution neural interfacing probes: materials and design approaches. *Nano Lett.* **19**, 2741–2749 (2019).
166. Wen, X. et al. Flexible, multifunctional neural probe with liquid metal enabled, ultra-large tunable stiffness for deep-brain chemical sensing and agent delivery. *Biosens. Bioelectron.* **131**, 37–45 (2019).
167. Lee, J. M. et al. Nanoenabled direct contact interfacing of syringe-injectable mesh electronics. *Nano Lett.* **19**, 5818–5826 (2019).
168. Taylor, D., Hazenberg, J. G. & Lee, T. C. Living with cracks: damage and repair in human bone. *Nat. Mater.* **6**, 263–268 (2007).
169. Gueorguiev, B. & Lenz, M. Cement augmentation and bone graft substitutes—Materials and biomechanics. *Unfallchirurg* **125**, 430–435 (2022).
170. Xu, H. H. K. et al. Calcium phosphate cements for bone engineering and their biological properties. *Bone Res.* **5**, 17056 (2017).
171. Stańczyk, M. & van Rietbergen, B. Thermal analysis of bone cement polymerisation at the cement–bone interface. *J. Biomech.* **37**, 1803–1810 (2004).
172. Hansen, E. Modelling heat transfer in a bone–cement–prosthesis system. *J. Biomech.* **36**, 787–795 (2003).
173. Shridhar, P. et al. A review of PMMA bone cement and intra-cardiac embolism. *Materials* **9**, 821 (2016).
174. Chang, T.-C., Wang, J.-W., Wang, M.-C. & Hon, M.-H. Solderability of Sn–9Zn–0.5Ag–1In lead-free solder on Cu substrate: Part 1. Thermal properties, microstructure, corrosion and oxidation resistance. *J. Alloy. Compd.* **422**, 239–243 (2006).
175. Zhang, Q. et al. Thermal evaluation of the injectable liquid metal bone cement in orthopedic treatment. *Sci. China Technol. Sci.* **63**, 446–458 (2020).
176. Quint, C. et al. Decellularized tissue-engineered blood vessel as an arterial conduit. *Proc. Natl. Acad. Sci. USA* **108**, 9214–9219 (2011).
177. L'Heureux, N., Pâquet, S., Labbé, R., Germain, L. & Auger, F. A. A completely biological tissue-engineered human blood vessel. *FASEB J.* **12**, 47–56 (1998).
178. Tamura, K. et al. Experimental application of polyvinyl alcohol-silica for small artificial vessels. *Biomater. Med. Devices Artif. Organs* **13**, 133–152 (1985).
179. L'Heureux, N. et al. Human tissue-engineered blood vessels for adult arterial revascularization. *Nat. Med.* **12**, 361–365 (2006).
180. Seifu, D. G., Purnama, A., Mequanint, K. & Mantovani, D. Small-diameter vascular tissue engineering. *Nat. Rev. Cardiol.* **10**, 410–421 (2013).
181. Cheng, S. et al. Self-adjusting, polymeric multilayered roll that can keep the shapes of the blood vessel scaffolds during biodegradation. *Adv. Mater.* **29**, 1700171 (2017).
182. Hoenig, M. R., Campbell, G. R., Rolfe, B. E. & Campbell, J. H. Tissue-engineered blood vessels: alternative to autologous grafts? *Arterioscler. Thromb. Vasc. Biol.* **25**, 1128–1134 (2005).
183. Cheng, S. et al. Electronic blood vessel. *Matter* **3**, 1664–1684 (2020).
184. Nadler, S., Weingand, K. & Kruse, R. The physiologic basis and clinical applications of cryotherapy and thermotherapy for the pain practitioner. *Pain. Physician* **7**, 395–399 (2004).
185. Wang, Y. et al. Printable Liquid-Metal@PDMS stretchable heater with high stretchability and dynamic stability for wearable thermotherapy. *Adv. Mater. Technol.* **4**, 1800435 (2019).

186. Sun, F. et al. Stretchable conductive fibers of ultrahigh tensile strain and stable conductance enabled by a worm-shaped graphene microlayer. *Nano. Lett.* **19**, 6592–6599 (2019).
187. Zhang, X. M., Yang, X. L. & Wang, K. Y. Conductive graphene/polydimethylsiloxane nanocomposites for flexible strain sensors. *J. Mater. Sci. Mater. Electron.* **30**, 19319–19324 (2019).
188. Lazarus, N. & Hanrahan, B. Thermotherapy platform based on a highly stretchable wireless heater. *Adv. Mater. Technol.* **1**, 1600130 (2016).
189. Tan, S. et al. Multifunctional flexible conductive filament for human motion detection and electrothermal.*Compos. Commun.* **37**, 101446 (2023).
190. Yun, G. et al. Liquid metal-filled magnetorheological elastomer with positive piezoconductivity. *Nat. Commun.* **10**, 1300 (2019).
191. Kong, K. & Jeon, D. Design and control of an exoskeleton for the elderly and patients. *IEEE ASME Trans. Mechatron.* **11**, 428–432 (2006).
192. Spina, F., Pouryazdan, A., Costa, J. C., Cuspinera, L. P. & Münzenrieder, N. Directly 3D-printed monolithic soft robotic gripper with liquid metal microchannels for tactile sensing. *Flex. Print. Electron.* **4**, 035001 (2019).
193. Berring, J., Kianfar, K., Lira, C., Menon, C. & Scarpa, F. A smart hydraulic joint for future implementation in robotic structures. *Robotica* **28**, 1045–1056 (2010).
194. Perry, J. C., Rosen, J. & Burns, S. Upper-limb powered exoskeleton design. *IEEE ASME Trans. Mechatron.* **12**, 408–417 (2007).
195. Deng, Y. & Liu, J. Flexible mechanical joint as human exoskeleton using low-melting-point alloy. *J. Med. Device* **8**, 044506 (2014).
196. Shu, J. et al. A liquid metal artificial muscle. *Adv. Mater.* **33**, 2103062 (2021).
197. Guo, H. et al. Fabrication of a flexible strain sensor with high-aspect-ratio liquid-metal Galinstan. *Adv. Mater. Technol.* **8**, 2200749 (2023).
198. Pei, X. et al. A bifunctional fully integrated wearable tracker for epidermal sweat and wound exudate multiple biomarkers monitoring. *Small* **18**, 2205061 (2022).
199. Yang, D. S., Ghaffari, R. & Rogers, J. A. Sweat as a diagnostic biofluid. *Science* **379**, 760–761 (2023).
200. Guo, C., Yu, Y. & Liu, J. Rapidly patterning conductive components on skin substrates as physiological testing devices via liquid metal spraying and pre-designed mask. *J. Mater. Chem. B* **2**, 5739–5745 (2014).
201. Guo, R. et al. Cu–EGaIn enabled stretchable e-skin for interactive electronics and CT assistant localization. *Mater. Horiz.* **7**, 1845–1853 (2020).
202. Gao, Y. et al. Wearable microfluidic diaphragm pressure sensor for health and tactile touch monitoring. *Adv. Mater.* **29**, 1701985 (2017).
203. Yeo, J. C., Yu, J., Koh, Z. M., Wang, Z. & Lim, C. T. Wearable tactile sensor based on flexible microfluidics. *Lab Chip* **16**, 3244–3250 (2016).
204. Li, T., Lv, Y.-G., Liu, J. & Zhou, Y.-X. A powerful way of cooling computer chip using liquid metal with low melting point as the cooling fluid. *Forsch. im. Ingenieurwesen* **70**, 243–251 (2005).
205. Xiang, S. et al. Liquid-metal-based dynamic thermoregulating and self-powered electronic skin. *Adv. Funct. Mater.* **31**, 2100940 (2021).
206. Filingeri, D., Zhang, H. & Arens, E. A. Characteristics of the local cutaneous sensory thermoneutral zone. *J. Neurophysiol.* **117**, 1797–1806 (2017).
207. Xu, Y. et al. Porous liquid metal–elastomer composites with high leakage resistance and antimicrobial property for skin-interfaced bioelectronics. *Sci. Adv.* **9**, eadf0575 (2022).
208. Tortorelli, P. F., Pawel, S. J. Corrosion by liquid metals in corrosion: fundamentals, testing, and protection (eds. Cramer S. D., Covino, B. S., Jr.) 220-227, (ASM International, 2003).
209. Park, Y.-G. et al. Liquid metal-based soft electronics for wearable healthcare. *Adv. Healthcare Mater.* **10**, 2002280 (2021).
210. Focus Technology Co., L. *Liquid Metal Price*. https://www.made-in-china.com/products-search/hot-china-products/Liquid_Metal_Price.html (2023).
211. Ping, B., Zhou, G., Zhang, Z. & Guo, R. Liquid metal enabled conformal electronics. *Front. Bioeng. Biotechnol.* **11**, 1118812 (2023).
212. Sun, X. et al. Nano-biomedicine based on liquid metal particles and allied materials. *Adv. NanoBiomed. Res.* **1**, 2170041 (2021).
213. Wang, L., Lai, R., Zhang, L., Zeng, M. & Fu, L. Emerging liquid metal biomaterials: from design to application. *Adv. Mater.* **34**, 2201956 (2022).
214. Hartmann, F. et al. Scalable microfabrication of folded parylene-based conductors for stretchable electronics. *Adv. Electron. Mater.* **7**, 2001236 (2021).
215. Bagchi, B. et al. Copper nanowire embedded hypromellose: An antibacterial nanocomposite film. *J. Colloid Interface Sci.* **608**, 30–39 (2022).
216. Xu, K. et al. Highly stable Kirigami-structured stretchable strain sensors for perdurable wearable electronics. *J. Mater. Chem. C.* **7**, 9609–9617 (2019).
217. Kyriakides, T. et al. Biocompatibility of nanomaterials and their immunological properties. *Biomed. Mater.* **16**, 042005 (2021).
218. Zhang, B. et al. Fully embedded CuNWs/PDMS conductor with high oxidation resistance and high conductivity for stretchable electronics. *J. Mater. Sci.* **54**, 6381–6392 (2019).
219. Yu, X.-G. et al. A wearable strain sensor based on carbonized nano-sponge/silicone composite for human motion detection. *Nanoscale* **9**, 6680–6685 (2017).
220. Park, W. et al. Advanced hybrid nanomaterials for biomedical applications. *Prog. Mater. Sci.* **114**, 100686 (2020).
221. Dhinesh Kumar, D. & Valan Arasu, A. A comprehensive review of preparation, characterization, properties and stability of hybrid nanofluids. *Renew. Sustain. Energy Rev.* **81**, 1669–1689 (2018).
222. Yang, H., Yan, J., Han, R., Wu, X. & Yang, S. Stretchable conductive hydrogel with super resistance-strain stability and ultrahigh durability enabled by specificity crosslinking strategy for high-performance flexible electronics. *Chem. Eng. J.* **465**, 142828 (2023).
223. Folorunso, O., Olukanmi, P. & Thokozani, S. Conductive polymers' electronic structure modification for multifunctional applications. *Mater. Today Commun.* **35**, 106308 (2023).

Acknowledgements

The authors acknowledge the financial support of the National Key Research and Development Program (2022YFE0121000), the National Natural Science Foundation of China (62288102), Natural Science Foundation of Shaanxi (Grant No. 5110210130), Key Research and Development Program of Shaanxi (Grant No. 5140220004) and Fundamental Research Funds for the Central Universities (Grant Nos. G2022WD01007 and D5000230125).

Author contributions

Y.D. collected the data and wrote the original manuscript with the assistance of F.B. and Y.W. The original draft was reviewed and edited by P.S.C., X.L., and C.G.

Competing interests

The authors declare no competing interests.

Additional information

Correspondence and requests for materials should be addressed to Pei Song Chee, Xiangye Liu or Cao Guan.